

**FORMULATION OF AN OPTIMAL
NON-TARGETED LIPOSOME PREPARATION
FOR FUSION WITH TUMOUR CELL LINE
MEMBRANES**

Ismail Mohammed Motala

2015

**Formulation of an optimal non-targeted liposome
preparation for fusion with tumour cell line
membranes**

By

Ismail Mohammed Motala

A mini dissertation submitted in fulfilment of the requirements for
the degree of Magister Scientiae (MSc) Nanoscience in the
Department of Biochemistry and Microbiology, Nelson Mandela
Metropolitan University

December 2015

Supervisor: Prof. Gareth Kilian
Co-supervisor: Prof. Saartjie Roux

Declaration

I, *Ismail Mohammed Motala*, hereby declare that the work entitled “*Formulation of an optimal non-targeted liposome preparation for fusion with tumour cell line membranes*” is my original work. It has not been submitted for any degree or examination in any other university and all the sources I have used or quoted have been indicated and acknowledged by complete references.

Ismail Mohammed Motala

Signature: _____

Signed on the _____ of _____ 2015

Dedication

I dedicate my dissertation work to my family. A special feeling of gratitude to my loving wife and daughter, Aisha and Juwairiyah for their patience and support throughout my studies. My parents, Mohammed and Mariam Motala whose words of encouragement and push for firmness ring in my ears. I also dedicate this dissertation to my sisters Swaleha, Salma and Sabiha for offering me encouragement and motivation in completing my studies.

Acknowledgments

- This paper could not be written to its fullest without Professor Gareth Kilian who served as my supervisor, as well as one who challenged and encouraged me throughout my time spent studying under him. He would have never accepted anything less than my best efforts, and for that, I thank him.
- I would also like to thank Professor Saartjie Roux who served as my co-supervisor, as well as one who throughout my studies has encouraged and motivated me in completing my studies. I thank her for her belief in me and her never ending inspiration.
- My heartfelt appreciation goes to the Department of Science and Technology (DST) for funding my studies as this dissertation wouldn't have been possible without their financial support.
- I would like to thank Nelson Mandela Metropolitan University (NMMU) for allowing me to complete my studies at the institute.
- I would like to thank Dr Hajierah Davids for offering me assistance with my cell culturing.
- I would like to thank Mrs Jean van Jaarsveld and Mrs Arista van Jaarsveld for assisting me and allowing me to utilise the pharmacy labs freely.
- I would finally like to thank Professor Maryna Van de Venter for assisting me in using the flow cytometer

Abstract

The most common treatment used for cancer is chemotherapy. Chemotherapeutic agents have a greater affinity for rapidly dividing cells which is a characteristic of tumour cells. Although anti-cancer agents have their advantages in providing anti-cancer effects, they can be seen as highly toxic molecules posing a threat to normal healthy tissue within the human body. However, these toxic therapies need to be delivered to tumour sites without damaging healthy tissue. Liposomes can serve as a delivery system for these toxic molecules and be delivered to the tumour site via the EPR effect. Hence, liposomes that fuse with tumour cell line membranes are advantageous in delivering payloads of drugs directly into the tumour cell without damaging normal healthy tissue.

The aim of the study was to formulate an optimised liposome preparation in order to enhance cellular uptake by MCF-7, Caco-2 and C3A cancer cell lines via membrane fusion. The optimal liposome formulation was aimed to be prepared utilising a statistical design approach in order to determine the ranges of the parameters that were furthestmost optimal in formulating an ideal liposome preparation.

The primary screening design was conducted using a 2^{4-1} fractional factorial design that took into account the four parameters that were used to determine the optimisation of the liposomal preparation. The four variables used in the liposome preparation were the phospholipid type (PS or DOPE), the concentration of cholesteryl hemisuccinate (CHEMS) (10 – 40 %), the concentration of PEG₂₀₀₀-PE (0.5 – 4 %) and liposome size (100 or 200 nm). Liposomes were prepared using thin film hydration method and characterisation for size and zeta potential was carried out

using photon correlation spectroscopy (PCS). Visual characterisation of liposome size was carried out using atomic force microscopy (AFM). Liposomes were exposed to the cancer cell lines with visualisation and uptake being measured using fluorescent microscopy and flow cytometry, respectively.

An optimal liposome preparation was prepared following the statistical design method. The optimal liposome preparation consisted of phospholipid type PS, 22.91 % of CHEMS, 4 % of PEG₂₀₀₀-PE and a liposome size of 200 nm. AFM analysis has shown that optimal liposome sizes ranged between 130 and 170 nm. Flow cytometry analysis indicated high level of liposome uptake with actual values falling below the predicted values set out by the statistical design. Fluorescence microscopy captured images of the fluorescent liposomes concentrated on the membrane of cells.

The objective of the study was to determine from literature which variables would be desirable in preparing an optimal non-targeted liposome preparation. This was achieved by identifying four such variables and utilising them in a statistical design approach which was screened in order to determine the ideal parameters in preparing the optimised liposome batch. Therefore, from the results obtained it can be concluded that the aim of the study were met by preparing an optimal liposome preparation that has the ability to fuse with the tumour cell line membranes.

Keywords

Nanotechnology, fusogenic liposomes, membrane fusion, cancer, MCF-7, Caco-2, C3A, optimisation, atomic force microscopy

TABLE OF CONTENTS

DECLARATION	I
DEDICATION	II
ACKNOWLEDGMENTS	III
ABSTRACT	IV
KEYWORDS	V
ABBREVIATIONS.....	XI
LIST OF SYMBOLS.....	XII
LIST OF FIGURES.....	XIII
LIST OF TABLES	XVI
CHAPTER 1: INTRODUCTION	1
1.1 BACKGROUND INFORMATION.....	1
1.2 AIM AND OBJECTIVES	4
1.2.1 AIM OF THE STUDY	4
1.2.2 OBJECTIVES OF THE STUDY	4
CHAPTER 2: LITERATURE REVIEW	5

2.1 OVERVIEW OF NANOTECHNOLOGY	5
2.1.1 NANOTECHNOLOGY IN MEDICINE	7
2.1.2 NANOTECHNOLOGY IN CANCER DRUG DELIVERY	8
2.1.3 NANOPARTICLES USED IN DRUG DELIVERY.....	9
2.1.3.1 CARBON NANOTUBES.....	10
2.1.3.2 DENDRIMERS	12
2.1.3.3 POLYMERIC NANOPARTICLES	14
2.1.4 NANOTECHNOLOGY IN DIAGNOSTICS	16
2.1.5 ADVANTAGES OF NANOPARTICLES	18
2.2 GENERAL INFORMATION ON LIPOSOMES.....	19
2.2.1 OVERVIEW OF LIPOSOMES AND ADVANTAGES	19
2.2.2 STRUCTURAL COMPONENTS OF LIPOSOMES.....	21
2.2.3 STRUCTURAL CLASSIFICATION OF LIPOSOMES.....	24
2.2.4 FUNCTIONAL CLASSIFICATION OF LIPOSOMES.....	26
2.2.5 METHODS OF LIPOSOME PREPARATION.....	29
2.2.6 APPLICATION OF LIPOSOMES.....	31

2.2.7	INTERACTION OF LIPOSOMES WITH CELLS.....	33
2.2.8	LIPOSOMES IN DRUG DELIVERY	34
2.3	CELL CULTURE MODELS	37
2.3.1	THE USE OF CELL CULTURE MODELS	37
2.3.2	MCF-7 CELL LINE.....	37
2.3.3	CACO-2 CELL LINE	38
2.3.4	C3A HEPATOCYTES CELL LINE.....	39
	CHAPTER 3: METHODOLOGY	40
3.1	MATERIALS	40
3.2	LIPOSOME PREPARATION	40
3.2.1	EXPERIMENTAL DESIGN	41
3.3	LIPOSOME CHARACTERISATION	44
3.3.1	ZETA POTENTIAL AND PARTICLE SIZE ANALYSIS	44
3.3.2	ATOMIC FORCE MICROSCOPY (AFM)	44
3.4	CELL CULTURING.....	45
3.4.1	HANDLING PROCEDURE FOR FROZEN CELLS.....	45

3.4.2	CELL GROWTH MEDIUM	46
3.5	INTRACELLULAR DELIVERY OF LIPOSOMES	47
3.5.1	FLUORESCENCE MICROSCOPY	47
3.5.2	FLOW CYTOMETRY ANALYSIS	47
3.6	STATISTICAL METHODS	48
CHAPTER 4: RESULTS AND DISCUSSION		49
4.1	BATCH OPTIMISATION EXPERIMENTS	49
4.1.1	CHARACTERISATION OF LIPOSOMES	49
4.1.1.1	PHOTON CORRELATION SPECTROSCOPY	49
4.1.2.1	FLOW CYTOMETRY ANALYSIS	51
4.1.2.1.1	UPTAKE INTO CELL LINES	51
4.2	STATISTICAL OPTIMISATION	54
4.2.1	LIPOSOME UPTAKE INTO MCF-7 CELL LINES	54
4.2.2	LIPOSOME UPTAKE INTO CACO-2 CELL LINES	59
4.2.3	LIPOSOME UPTAKE INTO C3A CELL LINES	61
4.3	OPTIMISED BATCH CHARACTERISATION	66

4.3.1 LIPOSOMAL UPTAKE INTO THE MCF-7, CACO-2 AND C3A CANCER CELL LINES	66
4.3.2 CHARACTERISATION OF LIPOSOMES.....	67
4.3.2.1 PHOTON CORRELATION SPECTROSCOPY	67
4.3.2.2 ATOMIC FORCE MICROSCOPY (AFM)	68
4.3.3 INTRACELLULAR DELIVERY OF LIPOSOME	70
4.3.3.1 FLOW CYTOMETRY ANALYSIS	70
4.3.3.2 FLUORESCENCE MICROSCOPY ANALYSIS	73
CHAPTER 5: CONCLUSIONS AND RECOMMENDATIONS	79
REFERENCES.....	81

Abbreviations

2FI	2 Factor interaction
6MP	6-mercaptopurine
AFM	Atomic force microscopy
Au-NPs	Gold nanoparticles
CHEMS	Cholesteryl hemisuccinate
CT	Computed tomography
DMEM	Dulbecco's modified eagle medium
DNA	Deoxyribonucleic acid
DOPE	1,2-dioleoyl-sn-glycero-3-phosphoethanolamine
DOTAP	1,2-dioleoyl-3-trimethylammonium-propane
DOTMA	1,2-di-O-octadecenyl-3-trimethylammonium propane
EMEM	Eagle's minimal essential medium
EPR	Enhanced permeability and retention
FACS	Fluorescence-activated cell sorting
FBS	Fetal bovine serum
MLV	Multilamellar vesicle
MRI	Magnetic resonance imaging
MWCNT	Multi-walled carbon nanotubes
NEAA	Non-essential amino acid
NMMU	Nelson Mandela Metropolitan University
PAMAM	Poly(amidoamine)
PBS	Phosphate buffered saline
PCS	Photon correlation spectroscopy
PE-CF	1,2-dioleoyl-sn-glycero-3-phosphoethanolamine-N-(carboxyfluorescein)
PEG ₂₀₀₀ -PE	1,2-dimyristoyl-sn-glycero-3-phosphoethanolamine-N-[methoxy(polyethylene glycol)-2000]
PEG	Polyethylene glycol
PET	Positron emission tomography
PS	Phosphatidylserine
RES	Reticuloendothelial system
RPMI	Roswell park memorial institute
SI	International System of Units
SUV	Small unilamellar vesicle
SWCNT	Single-walled carbon nanotubes

List of symbols

g	gram
M	molar
≈	approximately equal to
mg	milligram
min	minutes
H	hour
Mm	millimetre
mL	millilitre
mM	milimolar
μm	micrometre
Nm	nanometer (10 ⁻⁹ meters)
°C	degree celsius
>	greater than
<	less than
w/v	weight per volume
v/v	volume per volume
-	Minus
μl	micro litre
μM	micro molar
%	Percentage
Rpm	revolutions per minute
™	trademark

List of figures

Figure 1: Bucky ball (adapted from Boysen and Boysen, 2011).....	5
Figure 2: Single walled carbon nanotube (SWCNT) on left and multi-walled carbon nanotube (MWCNT) on right (adapted from Iijima, 2002; Peretz and Regev, 2012)	12
Figure 3: Representation of a dendrimer (adapted from Nanjwade <i>et al.</i> , 2009).....	13
Figure 4: Drug incorporation into nanocapsules and nanospheres (adapted from Jawahar and Meyyanathan, 2012)	16
Figure 5: Common nanoparticles used in nanomedicine imaging (adapted from Re <i>et al.</i> , 2012)	17
Figure 6: Illustration of the formation of liposomes and the lipid bilayer (adapted from Blomme, 2008).....	23
Figure 7: General structure of a phospholipid (adapted from (Cargillfoods, 2015) ..	23
Figure 8: Chemical structure of cholesterol	24
Figure 9: Chemical structure of CHEMS	24
Figure 10: Structures of different liposomes. (A) multilamellar vesicles, (B) large unilamellar vesicles, (C) small unilamellar vesicles, (D) multivesicular vesicles (Sharma and Sharma, 1997).....	26
Figure 11: Bangham thin-film hydration method (adapted from de Araújo Lopes <i>et al.</i> , 2013)	30

Figure 12: Schematic representation of intracellular delivery of liposomes in cells (adapted from Torchilin, 2005)	34
Figure 13: The above figure represents the pathways taken by liposomes via active targeting and passive targeting (adapted from Ghosh <i>et al.</i> , 2008).....	36
Figure 14: Overlay plots of the flow cytometry results for batches 1-8 performed on A: MCF-7, B: Caco-2 and C: C3A with the x-axis being the number of event and y- axis being the Mean fluorescence intensity (FL1 Log)	53
Figure 15: Predicted versus actual results for uptake of liposomes into MCF-7 cell line.....	55
Figure 16: One factor plots for variables in liposomal uptake in MCF-7 cell line	56
Figure 17: Interaction plots for variables in MCF-7 liposomal uptake	58
Figure 18: Predicted versus actual results for uptake of liposomes into Caco-2 cell line.....	59
Figure 19: One factor plots for variables in Caco-2 liposomal uptake	61
Figure 20: Predicted versus actual results for uptake of liposomes into C3A cell line	62
Figure 21: One factor plots for variables in C3A liposomal uptake	64
Figure 22: Interaction plot for variables in C3A liposomal uptake.....	65
Figure 23: Comparison of predicted and actual values of liposomal uptake into MCF- 7, Caco-2 and C3A cell lines	67

Figure 24: AFM image of the optimised liposome batch captured in noncontact mode.....	69
Figure 25: Graphical representation of the flow cytometry analysis of the optimal liposome preparation.....	72
Figure 26: Fluorescence microscopy of MCF-7 cell line treated with the optimal liposome preparation.....	74
Figure 27: Fluorescence microscopy of Caco-2 cell line treated with the optimal liposome preparation.....	75
Figure 28: Fluorescence microscopy of C3A cell line treated with the optimal liposome preparation.....	76

List of tables

Table 1: The most common natural/synthetic phospholipids used in liposome formation (adapted from Walde and Ichikawa, 2001)	22
Table 2: Structural classification of liposomes	25
Table 3: Representation of the quantity (mg) of lipid compositions used in preparing batches 1-8 and the optimal batch.	41
Table 4: Formulation parameters and levels for primary screening of liposome formulations using 2^{4-1} fractional factorial design.....	42
Table 5: Experimental runs for primary screening of optimal liposome preparation using 2^{4-1} fractional factorial design	43
Table 6: Representation of particle size, polydispersity index and zeta potential of experimental design batches 1-8	50
Table 7: Representation of the average mean fluorescence intensity (MFI) results for batches 1-8 in flow cytometry for MCF-7, Caco-2 and C3A cell lines.....	52
Table 8: Optimised liposome batch	65
Table 9: Representation of average particle size, polydispersity index and zeta potential of the optimised liposome batch	68
Table 10: Representation of the mean fluorescence intensity (MFI) results for the optimised liposome batch in flow cytometry for MCF-7 cell line.	71

Table 11: Representation of the mean fluorescence intensity (MFI) results for the optimised liposome batch in flow cytometry for Caco-2 cell line..... 71

Table 12: Representation of the mean fluorescence intensity (MFI) results for the optimised liposome batch in flow cytometry for C3A cell line. 71

Chapter 1: Introduction

1.1 Background information

Cancer is a universal term that is used to describe a large group of diseases that are caused by the creation and rapid growth of abnormal cells in the body. These cells are deemed abnormal, bearing in mind the fact that they grow outside their normal boundaries, thus causing harm to adjacent cells and other parts of the body. Metastasis occurs when cancer cells from the primary cancer site travel through the bloodstream or lymphatic system and begin to form new tumours in other parts of the body. The incidence of cancer worldwide in 2012 was estimated to be 14.1 million and for people who have died from cancer worldwide was 8.1 million (Cancer Research UK, 2015). It is estimated that by 2025, 19 million cases of cancer will be diagnosed each year. Some of the most common causes of cancer deaths worldwide are cancers of:

- Lung,
- Liver,
- Stomach,
- Colorectal, and
- Breast (National Cancer Institute, 2015).

Cancers can be treated in many ways such as radiotherapy, bone marrow transplants, vaccine therapy, immunotherapy, surgery and chemotherapy (National Cancer Institute, 2015). Although there are many methods of treatment for cancer, two of the most common treatments used worldwide are

chemotherapy and radiotherapy. These methods are used as second line treatments postoperatively. 'Chemotherapy' is a term that was invented by renowned researcher, Paul Ehrlich, in 1914 while searching for a substance to cure syphilis. However, today, the more common use of the term is to describe drugs that have a cytotoxic effect on tumour cells. Chemotherapeutic agents have a greater affinity for rapidly dividing cells which is a characteristic of tumour cells. There are over a hundred chemotherapeutic agents that are currently being used and there are new compounds being discovered frequently (Cancer Research UK, 2015). Oncologists have several factors to consider when deciding which chemotherapeutic agent is best suited to treat cancer patients. Some of these factors include:

- The type of cancer,
- The stage of cancer,
- Whether the cancer has metastasised, and
- The overall health of the patient.

Chemotherapy agents can be classified according to their chemical structure and mechanism of intracellular action. Alkylating agents are one of the oldest anti-cancer drugs used dating back to the early 1950s. They perform their function via covalent bonding of alkyl groups, mostly in DNA molecules, thus leading to cell death. Some of the most common alkylating agents include Cyclophosphamide, Ifosfamide and Temozolamide (Makin, 2014). Two common platinum compounds used as anti-cancer drugs are Cisplatin and Carboplatin. Their mechanism of cell death is similar to that of the alkylating agent. Antimetabolites are structurally related to intermediate molecules of cell metabolism such as folic acid, pyrimidine

or purine in protein and nucleic acid synthesis (Makin, 2014). They perform their function by incorporating themselves into these molecules, thus interfering with normal cell activity and cause cell death to the cancer cells (Makin, 2014). Examples of these common drug compounds are Methotrexate, 6-Mecaptopurine (6MP) and Fludarabine. These classes of anti-cancer drugs are just a few that have been named. Other classes that exist include steroids, topoisomerase inhibitors and tyrosine kinase inhibitors.

Although anti-cancer agents have their advantages in providing anti-cancer effects, they can be seen as highly toxic molecules. The toxicity of these molecules therefore poses a threat to normal, healthy tissue within the human body, particularly for rapidly dividing cells. Some of the common side effects experienced by cancer patients on chemotherapy include the following but are not limited to: haematological toxicity (Sjøblom *et al.*, 2015), neurotoxicity (Dietrich *et al.*, 2015), peripheral neuropathy (Carozzi *et al.*, 2015) and cardiac toxicity (Christenson *et al.*, 2015). Using a particulate drug delivery system where chemotherapeutic agents are encapsulated can protect healthy tissue from the undesirable toxic effects associated with these therapies. Liposomes, which are a concentric bilayer of phospholipids, have been studied extensively for this purpose and serve as a protective barrier and carrier for these toxic chemotherapy agents. By utilising nanotechnology in creating liposomes, chemotherapy will have the ability to be delivered to the tumour site, avoid healthy tissue and decrease the risk of chemotherapy induced toxicity.

1.2 Aim and objectives

1.2.1 Aim of the study

The aim of this research was to formulate and optimise a liposome preparation in order to enhance cellular uptake by cultured cancer cells via membrane fusion in order to better understand the factors that affect cellular uptake of these nanoparticles.

1.2.2 Objectives of the study

Based on the aim stated above, the objectives of this study are to:

- Determine the most suitable fusogenic lipids to be used in the liposome preparation from literature;
- Determine how liposome compositional variables influence uptake into MCF-7, Caco-2 and C3A cultured cell lines using a statistical design approach;
- Optimise and characterise an optimum liposome preparation for cellular fusion in order to enhance drug delivery.

Chapter 2: Literature review

2.1 Overview of nanotechnology

In December 1959, Nobel Prize winner, Richard P. Feynman, gave a fascinating speech titled, "There's Plenty of Room at the Bottom," in which he mentioned the future of miniaturisation (Feynman, 1960). In his speech he invited and challenged the audience to enter a new field of physics, well known to all of us today as nanotechnology. Ever since, nanotechnology has been a growing field and has expanded into various fields of sciences due to its benefits and capabilities.

The advent of nanotechnological discoveries began in 1985 at Rice University, Houston, where a team of well renowned researchers, Richard Smalley, Robert Curl and Harold Kroto, discovered C_{60} : Buckminsterfullerene also known as Bucky balls (Edwards, 2006, Kroto et al., 1985). Bucky balls consist of 12 pentagons and 12 hexagons within its structure (Figure 1). Findings like this led to subsequent discoveries which eventually steered Smalley and his team to achieve the Nobel Prize in chemistry in 1996. This was only the beginning of a new era in the scientific field.

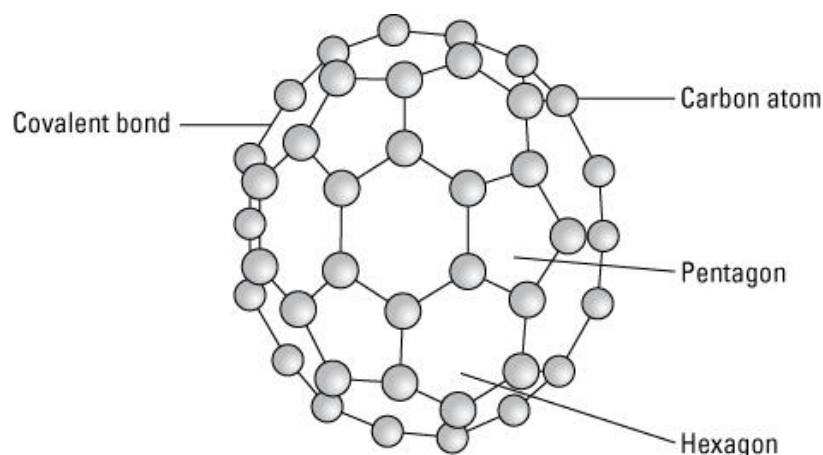


Figure 1: Bucky ball (adapted from Boysen and Boysen, 2011)

The name 'nanotechnology' derives from the Greek word 'nano' which means dwarf and is the SI prefix for one-billionth of a metre, 10^{-9} m. Nanotechnology is a scientific phenomenon that has exploded with interest in almost every constituent of the medicinal science and engineering fields. This is owing to the ability to allow characterisation, manipulation and fabrication of atoms at the nanoscale (Emerich and Thanos, 2003).

Nanotechnology is the gateway to many innovations in the above mentioned fields but the most important field that has really grasped the attention of scientists and researchers is the field of medicine. Nanotechnology gives researchers the cutting edge to explore its advantages and combine the physics behind the miniaturisation of particles and utilise them for medicinal purposes.

The advantages of nanotechnology were theorised by Richard Feynman in his speech where he made mention of the increased surface area at the nanoscale. He imagined printing a complete copy of the encyclopaedia on the head of a pin, which today is theoretically possible.

Another advantage is the scope at which nanotechnology functions (1-300 nm) that makes delivery into diseased cells considerably achievable. Nanoparticles can be functionalised or encapsulate molecules. These characteristics make them valuable in the medical field for therapeutics, diagnostics and prevention in diseased cells.

2.1.1 Nanotechnology in medicine

Nanomedicine is the application of nanotechnology for use in therapeutics, diagnostics, drug delivery and cell repair. The term 'nanomedicine' was first revealed in 1991 in a book called "Unbounding the Future: The Nanotechnology Revolution" (Drexler *et al.*, 1991). The authors described the need for new therapies and new approaches in healing diseased cells and tissues and mentioned nanomedicine as a backup system by building molecular devices which would destroy or omit what our immune systems cannot do during their natural healing processes. Nanomedicine can also be described as delivery structures in the nanometer size range that contain imaging agents, encapsulated drugs and targeting molecules for specific receptors (Koo *et al.*, 2005).

Nanomedicine is currently embarking on a journey to revolutionise the future of medicine. We are almost at an era where nanomedicine can be personalised to meet specific requirements in patients. Globally, cancer is one of the most common diseases with which researches are faced and tasked to find new therapies, early detection methods and successful diagnostics for (Gupta, 2011). Nanomedicine allows nano-sized particles to be injected into the blood stream without occluding needles and are advantageous in drug delivery and imaging in pathological diseases such as cancer, which also improves their pharmacokinetics (Koo *et al.*, 2005). Cancer is one of the most common causes of death worldwide making the disease a topic on many researchers' lists (Ferlay *et al.*, 2010). Nanomedicine promises to play a vital role in combating cancer as there are numerous benefits of nanotechnology. With this in mind, nanomedicine will be discussed with its use in cancer therapeutics, diagnostics and imaging.

2.1.2 Nanotechnology in cancer drug delivery

Nanomedicine can be used as a platform to deliver cancer drug molecules to tumour sites through the utilisation of nanoparticles. These nanoparticles are used as delivery vehicles to deliver drug molecules into tumour sites. Drug molecules can either be delivered via active targeting for specific receptors on tumour sites or they can be passively targeted through the enhanced permeability and retention (EPR) effect in the human body. An EPR effect occurs at tumour sites and is advantageous due to the leaky vasculatures of blood vessels supplying these rapidly growing tumours.

Drug delivery is an important component of medicine which has attracted a lot of interest by researchers worldwide. Due to the immense importance of the safety that has revolved around the delivery of drug molecules specific to tumour sites, researchers have begun to develop drug delivery systems (Orive *et al.*, 2003). Nanotechnology has the ability to improve the therapeutic index of current drug molecules on the market by decreasing their toxic effects on normal healthy tissue within the body by encapsulating them or targeting them to diseased cells; consequently, pharmaceutical companies show increasing interest in nanotechnology (Vasir *et al.*, 2005). Nanoparticles have been proven to be the safest and most reliable mode of transport for drug molecules as they have the ability to bypass normal healthy tissue and be delivered to the required site of action (Parveen *et al.*, 2012). Nanotechnology plays a vital role in the development of drug delivery methods in improving stability, bioavailability, and absorption of the desired drug molecules at the site of action (Sahoo *et al.*, 2007). The ultimate result of the above mentioned statement is that there is a rapid decrease of drug toxicity in normal,

healthy tissues compared to prior incorporation of nanoparticles as drug delivery vehicles (Koo *et al.*, 2005).

2.1.3 Nanoparticles used in drug delivery

The advent of nanoparticles was first described in 1976 by researchers Kreuter and Speiser after they prepared nanoparticles made of poly (methyl methacrylate) as an adjuvant (Kreuter and Speiser, 1976, Lee *et al.*, 2014). Following this discovery, there have been numerous others that have contributed to the field of nanotechnology and medicine. As previously discussed, nanoparticle usages are widespread in various diseases such as cancer, antimicrobial uses, inflammatory uses and vaccinations, making these nanoparticles an extraordinary discovery for researchers and pharmaceutical establishments. Nanoparticles have the ability to not only deliver drug molecules to sites of action but also may be functionalised for imaging and diagnostics. Nanoparticles such as quantum dots (QD) or gold nanoparticles (Au-NPs) are routinely used in cancer detection and cell imaging (Parveen *et al.*, 2012). The use of imaging and drug delivery together can be referred to with a widespread term called 'theranostics'. The benefits do not limit the use of nanoparticles in the medicinal fields, thus making them more intriguing in their usages and explorations.

Some of the most common nanoparticles that are being researched as drug delivery vehicles are carbon nanotubes, fullerenes, dendrimers, polymeric micelles, nanoshells and liposomes. Being in the nano-sized range, these nanoparticles have many advantages: they can be used for targeted drug delivery, they have the ability to encapsulate unstable drug molecules and be used for theranostic approaches

(Dawar *et al.*, 2013). Therefore, the above mentioned nanoparticles will be further discussed to gain an insight into their characteristics and uses in drug delivery.

2.1.3.1 Carbon nanotubes

In 1991, researcher Sumio Iijima was the first individual to synthesis carbon nanotubes, utilising an arc-discharge evaporation method, similar to that used to create fullerenes (C₆₀-Bucky balls) (Iijima, 1991). Carbon nanotubes have gained an increased interest in this research field due to their unique properties that researchers can exploit, such as mechanical, electrical, thermal, optical and structural properties (Tran *et al.*, 2009). Carbon nanotubes can be divided into two classes, single wall carbon nanotubes (SWCNT) and multi-walled carbon nanotubes (MWCNT). Carbon nanotube structures consist of graphene sheets that are rolled concentrically to form a tube-like structure. SWCNTs consists of diameter sizes ranging from 0.2 nm – 10 nm and MWCNTs consist of diameters between 2 nm – 100 nm with a length of about 0.2 µm – 5 µm (Figure 2) (Peretz and Regev, 2012). The three most common applications that carbon nanotubes are used for are encapsulating the drug in the walls of the nanotubes, adsorption of the drug molecules onto the surface of the carbon nanotubes and attaching the drug molecules to functionalised carbon nanotubes (Wilczewska *et al.*, 2012). The encapsulation method is the most suitable approach as the drug molecule is not exposed to degradation and it also allows for a triggered release (Perry *et al.*, 2011). With regard to their use in drug delivery, MWCNTs are the most suitable carbon nanotube due to their large surface area and multi-walled structure allowing for drug molecules to be incorporated inside the walls. MWCNTs are of concern due to their high density, thus this could result in toxicity levels in the body. Toxicities of carbon

nanotubes are of concern to scientists as these nanocarriers have the ability to become toxic at high levels in the body. Their toxicity depends on several factors such as:

- Carbon nanotube structure (size, shape, length),
- Production method, and
- Carbon nanotube functionalization (covalent or non-covalent) (Peretz and Regev, 2012).

There are studies that have been conducted using SWCNTs for targeted drug delivery into colorectal cancers (Lee *et al.*, 2013). In this study SN38 (7-ethyl-10-hydroxycamptothecin), a topoisomerase I inhibitor was covalently linked to the SWCNT via a carbamate linker to treat colorectal cancer. The scientists found that the modified SWCNTs entered the tumour cells and detached, thus releasing the SN38 drug molecule intracellularly for anti-tumour activity (Lee *et al.*, 2013). Just like all nanoparticles, carbon nanotubes, when delivered into the blood stream, have been shown to be cleared via the reticular endothelial system (RES) (Schipper *et al.*, 2008). Thus, researchers have successfully functionalised SWCNTs with branched poly (ethylene glycol) (PEG) chains in order to increase their bioavailability and avoid the RES (Tran *et al.*, 2009).

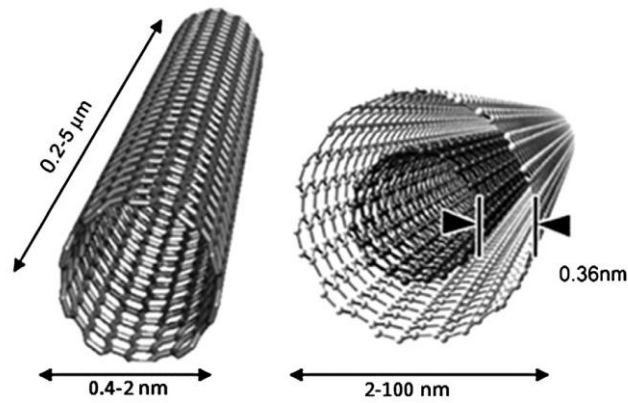


Figure 2: Single walled carbon nanotube (SWCNT) on left and multi-walled carbon nanotube (MWCNT) on right (adapted from Iijima, 2002; Peretz and Regev, 2012)

2.1.3.2 Dendrimers

In 1985, Donald A. Tomalia and his team of scientists revealed their new discovery, the synthesis of “starburst polymers” also known as dendrimers (Tomalia *et al.*, 1985). Dendrimers are polymeric molecules that consist of monomers that branch from the core which consists of three architectural domains (Figure 3):

- the multivalent surface,
- the interior shells surrounding the core, and
- the core to which the dendrons are attached (Parveen *et al.*, 2012).

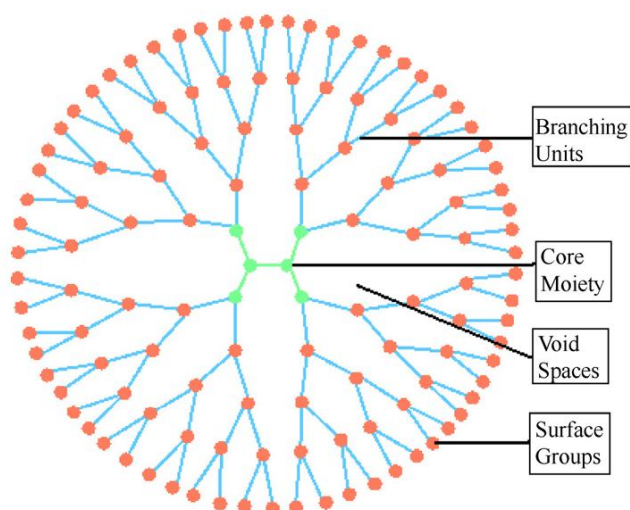


Figure 3: Representation of a dendrimer (adapted from Nanjwade *et al.*, 2009)

These domains allow for dendrimers to be constructed in a manner that they may be utilised as sensors and drug carriers. In addition, the terminal groups of dendrimers can be modified in order to change the dendrimers' solubility effects; for example, the hydrophobic terminal groups can make a dendrimer with a hydrophilic core oil soluble, while a hydrophilic terminal group can make a dendrimer with a hydrophobic core more water soluble (Liu *et al.*, 2000). Dendrimer size ranges between 1 nm – 100 nm making them versatile in drug delivery as they can evade the RES, prolonging their circulation time and allowing for controlled drug release (Gupta *et al.*, 2006).

Post synthesis of the dendrimers, researchers have utilised these fascinating dendrimers in many fields of medicine. This is due to these macromolecules having a high functionality, and being multi-branched with a three dimensional structure (Bhadra *et al.*, 2003). The most common dendrimer is poly (amido amide) (PAMAM) which is frequently used in biomedical applications (Wilczewska *et al.*, 2012). Drug molecules are delivered into the body via two methods:

- incorporation of drug molecules into dendrimer structure, or
- surface functionalisation of the dendrimers.

Attachment of drug molecules onto the dendrimers are carried out with the aid of hydrogen bonding, van de Waals forces and electrostatic interactions between both drug molecule and dendrimer (Svenson, 2009). Dendrimers are being researched as drug delivery vehicles on three main drug classes, which are: anti-inflammatories, anti-cancer, and anti-malarial drugs (Svenson, 2009). In the past, dendrimers have been successfully used to transfect cells for gene delivery (Zhang *et al.*, 2007). Due to the easy passage of dendrimers across biological barriers for drug delivery, dendrimers have been studied for various routes of administration such as: oral drug delivery, transdermal drug delivery and ocular drug delivery (Nanjwade *et al.*, 2009). In a study conducted by Navid Malik and his team of scientists, they successfully conjugated an anti-cancer drug molecule, cisplatin, onto a dendrimer which resulted in various advantages over free cisplatin (Malik *et al.*, 1999). Some of the advantages were slower drug release, increased accumulation in tumours and decreased toxicity in normal tissue.

2.1.3.3 Polymeric nanoparticles

Polymeric nanoparticles are spherical in shape and range in diameter from 10 nm – 100 nm and are composed of decomposable or biocompatible polymers and copolymers (Safari and Zarnegar, 2014). The biocompatibility of these nanoparticles allows researchers to utilise them in drug delivery where toxicity of nanoparticles are

of concern. Drug molecules can be incorporated into these nanoparticles via three methods:

- encapsulated into the nanoparticle,
- absorbed onto the surface of the nanoparticle, or
- chemically linked to the nanoparticle (Kuo and Chen, 2006, Parveen *et al.*, 2012).

Polymeric nanoparticles can be divided into two types, nanocapsules and nanospheres, depending on their method of manufacture. A nanosphere comprises of a polymer matrix and has the ability to entrap drug molecules or adsorb them onto the nanoparticle's surface. A nanocapsule contains a core sheltered by a polymer which allows drug molecules to be encapsulated within (Figure 4) (Parveen *et al.*, 2012).

Polymeric nanoparticles have been successfully used in a study where researchers incorporated an anti-neoplastic agent into a natural biodegradable polymer containing sodium alginate (Nanjwade *et al.*, 2010). The anti-neoplastic agent, being carboplatin, was targeted to the tumour site successfully. It was found that not only did the polymeric nanoparticle aid in drug delivery, but less of the drug was found in normal, healthy tissue. Thus, this substantiates that nanoparticles can be used for drug delivery of anti-neoplastic agents.

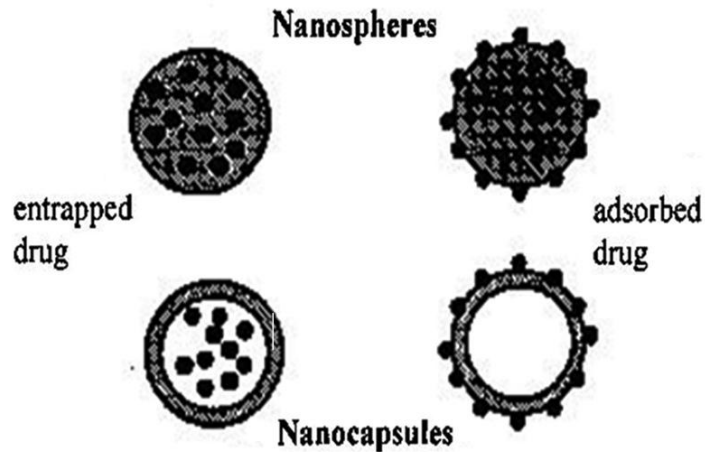


Figure 4: Drug incorporation into nanocapsules and nanospheres (adapted from Jawahar and Meyyanathan, 2012)

2.1.4 Nanotechnology in diagnostics

After the advent and success of nanotechnology in therapeutics, scientists have begun to utilise nanoparticles in imaging and detection of diseased cells, mainly in cancer. Imaging of these diseased cells utilising nanotechnology can be carried out using certain imaging techniques which comprise of positron emission tomography (PET), magnetic resonance imaging (MRI), fluorescence microscopy, computed tomography and ultrasound (Koo *et al.*, 2005). The most common nanoparticles that are being used in nanotechnology imaging research can be seen in Figure 5. It is important to note that in order to attain the desired outcomes of these nanosystems for imaging; they need to be designed in a manner that allows them easy passage into tumours or diseased cells.

The most interesting nanoparticle for imaging studies from Figure 5 is quantum dots. Quantum dots are semiconductor nanocrystals that were discovered in the early 1980s by scientists, Louis Brus and Alexi Ekimov, independently (Ekimov *et al.*, 1985, Yan *et al.*, 2011). Quantum dots have the required design and characteristics

that researchers need when utilising them in imaging studies. Their size, in diameter, ranges from 5 nm – 20 nm depending on type and manufacturing process of the quantum dots. These nanoparticles are composed of group II-VI or III-V elements from the periodic table and are said to have physical dimensions that are smaller than the exciton Bohr radius (Chan *et al.*, 2002). This enables these nanoparticles to be fluorescent when excited at their respective wavelengths; excitations at shorter wavelengths are possible in these nanoparticles. The optical properties of the quantum dots allows for state-of-the-art imaging, such as multiplexing.

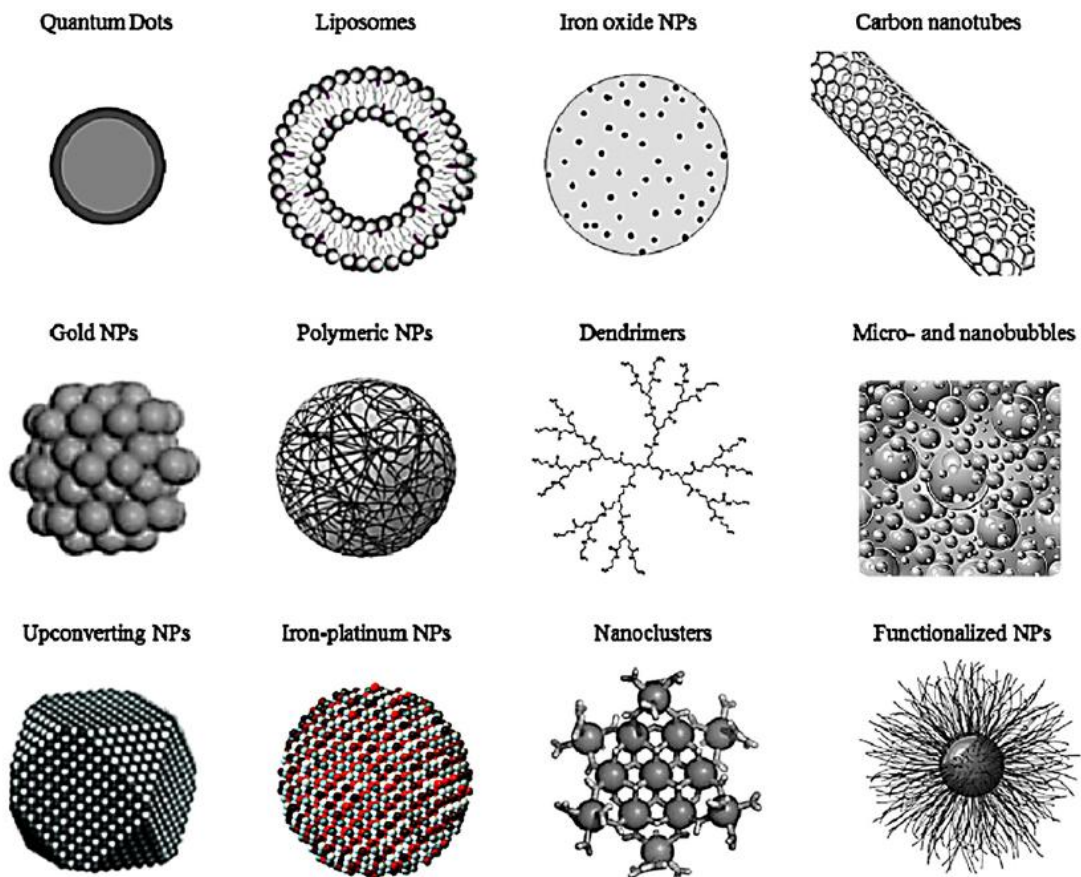


Figure 5: Common nanoparticles used in nanomedicine imaging (adapted from Re *et al.*, 2012)

Therefore, this permits quantum dots such as ZnS capped with CdSe to be excited at wavelengths as short as 13 nm between 18 °C and 23 °C (Chan and Nie, 1998).

Multiplexing research was carried out by Han and co-workers in which they analysed genes and proteins utilising quantum dots of varying sizes that made them fluorescent at different wavelengths (Han *et al.*, 2001). CdSe quantum dots were to encrypt proteins and nucleic acid sequences via the linkage of peptides, proteins and oligonucleotides to the quantum dots. In another study carried out by Ciaran and co-workers, quantum dots composed of cadmium telluride were coated with gelatine and heparin was attached to the surface of these quantum dots (Maguire *et al.*, 2014). These modified quantum dots were researched on Caco-2 cell lines for imaging and heparin was used as a stabilising agent for the quantum dots. The results have shown that the quantum dots were internalised and these quantum dots can be utilised for further cancer imaging studies.

2.1.5 Advantages of nanoparticles

Thus far nanoparticles have proven to be a thriving discovery in the scientific field for scientists who are researching better or more effective methods of drug delivery, imaging and theranostic approaches. There are various advantages that have been observed with these fascinating particles. Some of the advantages have already been exploited by pharmaceutical companies and thus we have seen anti-cancer agents being administered with nanoparticles (de la Fuente *et al.*, 2014). Some of the most common advantages of the above mentioned nanoparticles are:

- ability to encapsulate hydrophobic/hydrophilic drug molecules,
- longer circulation time in the body,

- ability to target specific receptors for targeted imaging or drug delivery,
- ability to achieve imaging and therapeutic effects simultaneously,
- larger surface area resulting in an increased drug loading, and
- they are also biocompatible and biodegradable.

However, this study focuses on reducing the complexity and cost of producing a liposomal drug delivery system that will have the ability to encapsulate anti-cancer molecules that are not drug and tumour specific.

2.2 General information on liposomes

2.2.1 Overview of liposomes and advantages

Liposomes were first discovered by Alec Bangham in the early 1960s (Bangham *et al.*, 1965) and ever since liposomes have undergone extensive research in the field of nanotechnology and resulted in numerous applications for use in cancer therapy and tumour imaging (Hauert and Bhatia, 2014). In brief, liposomes are concentric bi-layered vesicles that are made up of phospholipids and usually cholesterol. Liposomes have the ability to entrap drug molecules within its structure making them extensively researched for their use in cancer therapies. They have the ability to entrap both hydrophobic and hydrophilic molecules in their aqueous core or lipid bilayers (Gupta, 2011). This allows researchers to take full advantage of this phenomenon and deliver hydrophobic and/or hydrophilic drug molecules to diseased cells such as cancer.

Liposomes sizes ranges from about 1 μm for multilamellar vesicles to 20 nm for small unilamellar vesicles depending on the method of production and nature of their

use (Torchilin, 2005). The different methods of production of liposomes are reverse phase evaporation, freeze-thaw, pH-jump and thin film hydration methods. These methods have been used successfully by researchers to produce liposomes of desired sizes and compositions. Liposomes can be classified according to their structure ranging from small unilamellar vesicles to multilamellar vesicles. The functional uses of liposomes further classifies them in accordance with their composition and in what way they deliver encapsulated molecules to diseased tissues and cancers. These liposomes are termed conventional (Cattel et al., 2002, Gerasimov et al., 1999), long circulating (Deol and Khuller, 1997), immuno-liposomes (Park *et al.*, 2001), cationic (Shim *et al.*, 2013), pH sensitive (Simoes *et al.*, 2001) and fusogenic (Düzgüneş and Nir, 1999).

Liposome research has been ground breaking for scientists due to their vast array of advantages. The important advantage of liposomes is that they increase the therapeutic index of toxic drugs via drug encapsulation and have the ability to increase the stability of unstable drug molecules. Anti-cancer drug molecules pose a challenge to clinical researchers due to their toxicity to normal healthy tissues when being administered unaided (Sawant and Torchilin, 2012). Thus, the use of liposomes in encapsulating these toxic drug molecules has greatly been advantageous moving cancer therapy forward. In addition, the most common, well known advantages of liposomes are that they are biodegradable, non-toxic, non-immunogenic and multifunctional (Akbarzadeh *et al.*, 2013).

2.2.2 Structural components of liposomes

Liposomes are composed of biocompatible or biodegradable material that is made up of natural or synthetic phospholipids and a sterol membrane stabilising agent such as cholesterol or its derivatives. These phospholipids are responsible for the formation of the lipid bilayer which is the main structural characteristic of liposomes.

Phospholipid structures consist of a polar head (hydrophilic) and a non-polar tail (hydrophobic) which are amphiphilic in nature and are responsible for forming the lipid bilayers in liposomes (Figure 6) (Blomme, 2008). The general structure of a phospholipid contains a polar head group, a phosphate neck, a glycerol back-bone and a fatty acid chain. The polar head group comes into direct contact with the aqueous interior when the liposome is formed, while the non-polar tail assembles itself to form the interior of the lipid bilayer (Walde and Ichikawa, 2001). The natural/synthetic phospholipids described in Table 1 below can be divided into three types: zwitterionic (neutral), cationic (positive) and anionic (negative) charged phospholipids (Walde and Ichikawa, 2001). This allows researchers to utilise these lipids for the desired applications of the liposomes in gene transfections, fusion of liposomes with cell membranes and destabilisation of liposomal membranes at acidic pH.

Table 1: The most common natural/synthetic phospholipids used in liposome formation (adapted from Walde and Ichikawa, 2001)

<u>Natural</u>	<u>Synthetic</u>
Phosphatidyl choline (Lecithin) - PC	Dipalmitoylphosphatidylcholine – DPPC
Phosphatidyl ethanolamine (cephalin) - PE	1,2-Dioleoyl- sn-glycero-3-phosphoethanolamine – DOPE
Phosphatidyl serine (bovine) – PS	1,2-Dioleoyl- sn-glycero-3-phosphoethanolamine – DOTAP

Cholesterol and its derivative, cholesteryl hemisuccinate (CHEMS) (Figures 8 and 9), are the most common stabilising agents that are used in liposomes in order to increase their rigidity and allow for robust encapsulation of drug molecules. They also enhance the liposomes' resistance to degradation and aggregation between liposomal carriers (Yang *et al.*, 2013). The chemical modification of CHEMS allows this sterol to adopt a lamellar ordered phase in aqueous media, whereas cholesterol arranges into monohydrate crystals in an aqueous environment (Lai *et al.*, 1985a, Renshaw *et al.*, 1983).

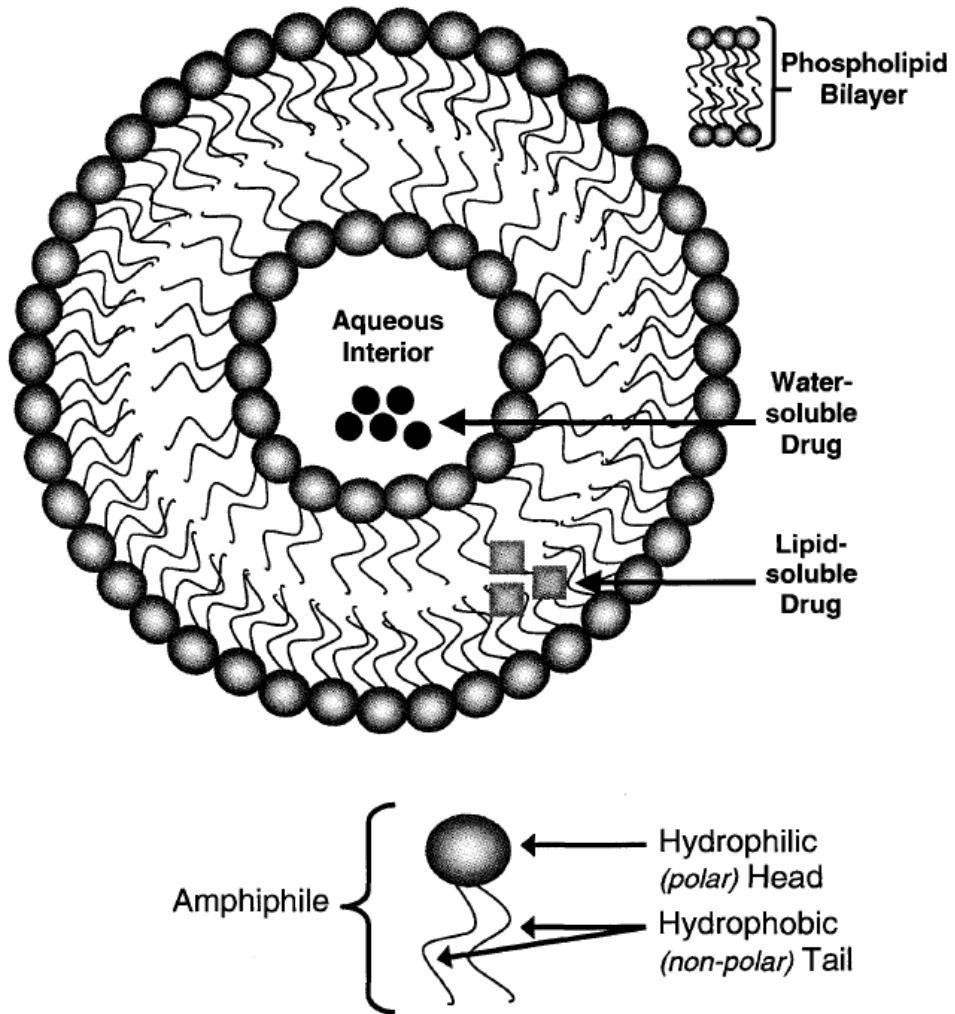


Figure 6: Illustration of the formation of liposomes and the lipid bilayer (adapted from Blomme, 2008)

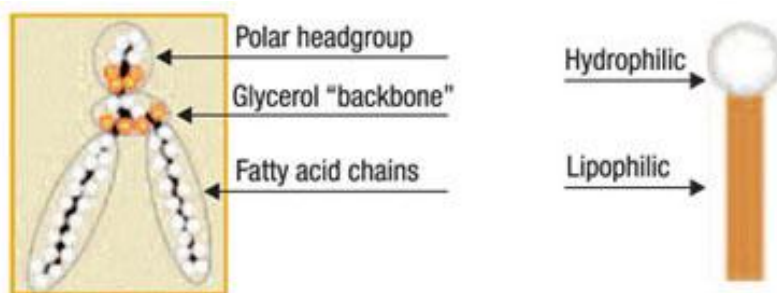


Figure 7: General structure of a phospholipid (adapted from Cargillfoods, 2015)

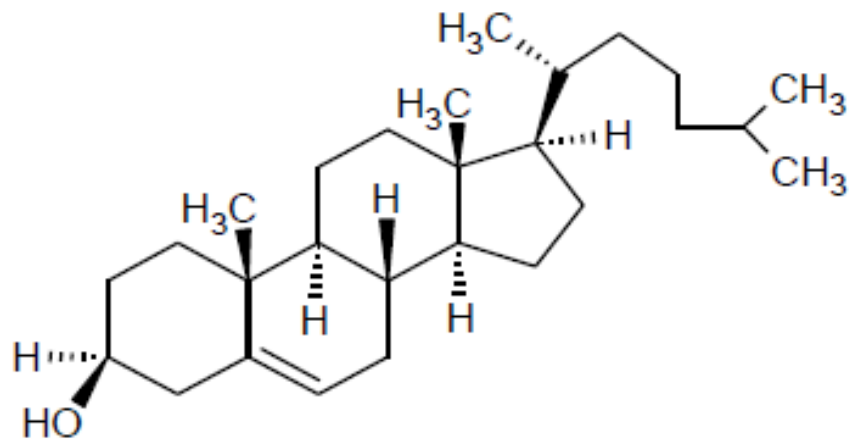


Figure 8: Chemical structure of cholesterol

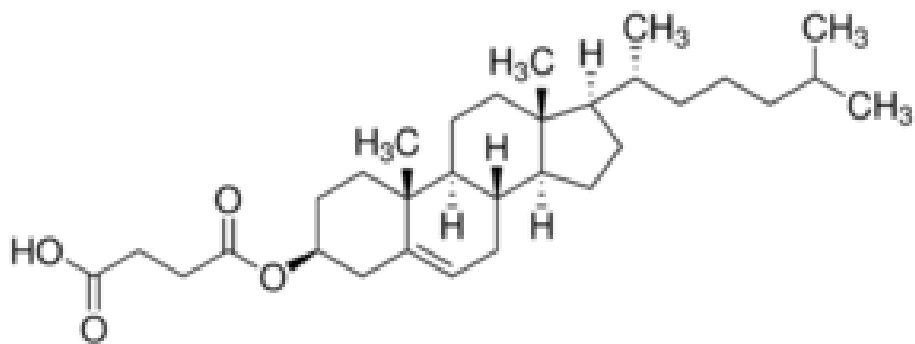


Figure 9: Chemical structure of CHEMS

2.2.3 Structural classification of liposomes

Liposomes can be classified either based on their structural parameters such as size and shape or by the method of their production. The structural parameters are described in Table 2 below (Alexis *et al.*, 2008, Emanuel *et al.*, 1996, Torchilin, 2005). The size determines the half-life or circulation time and distribution of the

liposomes. The number of vesicle membranes (Figure 10) is important in assisting with the extent of drug molecules that need to be encapsulated (Sharma and Sharma, 1997). The structure of unilamellar liposomes can be described as a single phospholipid bilayer that encompasses an aqueous solution. While a multilamellar vesicle consists of various lipid bilayers that enclose an aqueous core and a multivesicular liposome consists of different sizes of liposomes enclosed by a large unilamellar vesicle.

Table 2: Structural classification of liposomes		
Type	Diameter size	No. of lipid bilayers
Small unilamellar vesicles	20 – 100 nm	Single lipid bilayer
Large unilamellar vesicles	≥ 100 nm	Single lipid bilayer
Oligolamellar vesicles	0.1 – 1 μm	Two to ten lipid bilayers
Multilamellar vesicles	≥ 1 μm	Several lipid bilayers
Multivesicular vesicles	20 nm - ≥ 1 μm	Several lipid vesicles

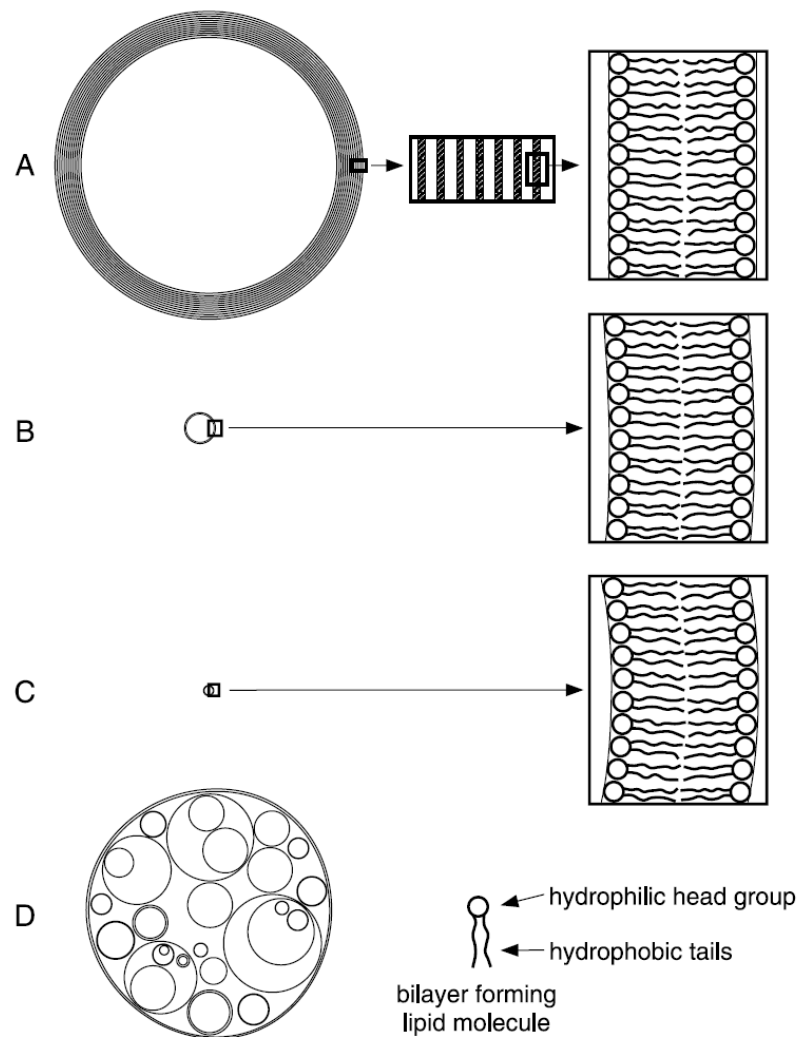


Figure 10: Structures of different liposomes. (A) multilamellar vesicles, (B) large unilamellar vesicles, (C) small unilamellar vesicles, (D) multivesicular vesicles (Sharma and Sharma, 1997)

2.2.4 Functional classification of liposomes

Liposomes can be classified in accordance with their lipid composition such as the different phospholipids and their functionalities via attachments of targeting peptides or long circulating molecules onto the surface of the liposomes. These include conventional (Cattel et al., 2002, Gerasimov et al., 1999), long circulating (Deol and Khuller, 1997), immuno-liposomes (Park *et al.*, 2001), cationic (Shim *et al.*, 2013), pH sensitive (Simoes *et al.*, 2001) and fusogenic liposomes (Düzgüneş and Nir, 1999).

Conventional liposomes are the first generation of liposomes that were made and are usually made up of neutral or negatively charged lipids which make use of cholesterol as the stabilising agent (Gerasimov *et al.*, 1999). However, conventional liposomes encounter various problems with biodistribution, plasma stability and blood circulation time (Cattel *et al.*, 2002). In 1982, Gabizon and co-workers successfully encapsulated the anticancer agent doxorubicin. The authors mentioned that they utilised negatively and neutral charged phospholipids to make the liposomes which decreased the cardiotoxicity related issues with the anticancer drug (Gabizon *et al.*, 1982). This is just one of many successful uses of conventional liposomes in the fight for cancer.

After the advent of first generation liposomes, researchers have found that the conventional liposomes were being rapidly eliminated *in vivo* by the reticular endothelial system (RES). This prompted further research to decrease the rapid elimination of these liposomes, which led to the discovery of reduced recognition of liposomes with poly(ethylene)glycol polymer (PEG) attached to its surface (Fonseca *et al.*, 2014). Thus, this resulted in an increase in their circulation time due to the PEG aiding the liposomes in evading the RES. This discovery led to the formulation of 2nd generation liposomes, also known as STEALTH® liposomes which have been extensively studied (Drummond, D. C. *et al.*, 1999).

Targeting liposomes were developed since conventional and long-circulating liposomes were ultimately being cleared by the RES due to their non-specificity. Immuno-liposomes consist of both conventional and long-circulating liposomes with

the added benefit of an attached targeting peptide or anti-body to the surface of the liposomes. Immuno-liposomes deliver drugs directly to the site of action such as tumours and diseased tissues via active targeting (Lasic and Papahadjopoulos, 1996, ElBayoumi and Torchilin, 2010).

Cationic liposomes are made-up of positively charged lipids such as dioleoyltrimethylammonium propane (DOTAP) or dioleoyloxypropyl-trimethylammonium chloride (DOTMA) (Düzgüneş and Nir, 1999). Early studies have shown that the use of these lipids have aided in intracellular delivery of encapsulated molecules via membrane fusion with cells (Magee *et al.*, 1974). Neutral lipids such DOPE and cholesterol are also used in conjunction with cationic liposomes to assist in delivery efficiencies as well as increase the rigidity of the liposomes to degradation (*Shim et al.*, 2013).

pH sensitive liposomes become active and release their encapsulated molecules when they come into contact with an acidic pH at the targeted site. They may also be referred to as stimuli-sensitive liposomes. pH sensitive liposomes are composed of lipids such as DOPE, which is termed a helper lipid, and an acidic lipid such as CHEMS (Cullis and De Kruijff, 1978, Lai *et al.*, 1985b). DOPE is used due its ability to destabilise the liposomal membrane at acidic pH and assist with endosomal membrane fusion (Hafez and Cullis, 2001).

Liposomes that fuse with cell membranes are subject to intense research due to their ability to permit intracellular delivery of encapsulated molecules. Fusogenic liposomes have the ability to deliver payloads of molecules that are impermeable to

cellular membranes or toxic to normal cells, such as hydrophilic drugs, proteins and genes (Kono et al., 2000, Torchilin, 2005, Torchilin, 2012). There are various factors that hinder the ability of liposomes to fuse with cell membranes, some of which are: (a) types of lipids, (b) lipid concentrations, (c) the phase transition state of the liposomal membrane, (d) circulation period, and (e) liposome size.

2.2.5 Methods of liposome preparation

Several methods of liposome production have been reported in literature such as: thin film hydration, reverse phase evaporation, pH jump method, and freeze thaw methods, just to name a few. The most common method of preparation of liposomes is the thin film hydration method which produces multilamellar vesicle (MLV) liposomes (Sharma and Sharma, 1997). The thin film hydration method was first proposed by Bangham and co-workers in 1965 and, ever since, this method has been used extensively by researchers (Bangham *et al.*, 1965). With the thin film hydration method, the desired lipids are dissolved in an organic solvent such as chloroform and methanol to produce a homogenous mixture of the lipids. Usually, 10 mg lipid mixture per 1 ml of solvent is used. The solvent is then evaporated via two methods depending on the amount of solvent used. They can either be flushed with nitrogen gas or using rotary evaporation with larger amounts of solvent. This then produces a clear-like film at the bottom of a round bottom glass flask which can then be hydrated with a saline solution such as phosphate buffer at pH 7.4 in a shaking water bath. This ultimately produces a heterogeneous mixture of multilamellar vesicles (MLVs) and small unilamellar vesicles (SUVs) which need to be further extruded or sonicated to a desired size distribution (Figure 11) (Dua *et al.*, 2012).

Reverse phase evaporation is another common method of liposome preparation where a water-in-oil emulsion is sonicated with the phospholipid and organic solvent and evaporated under reduced pressure. The organic mixture usually used is made up of diethylether or isopropyl ether or a mixture of isopropyl ether and chloroform (Dua *et al.*, 2012). The liposomes are formed when the gel emulsion and residual solvent is rotary evaporated under reduced pressure.

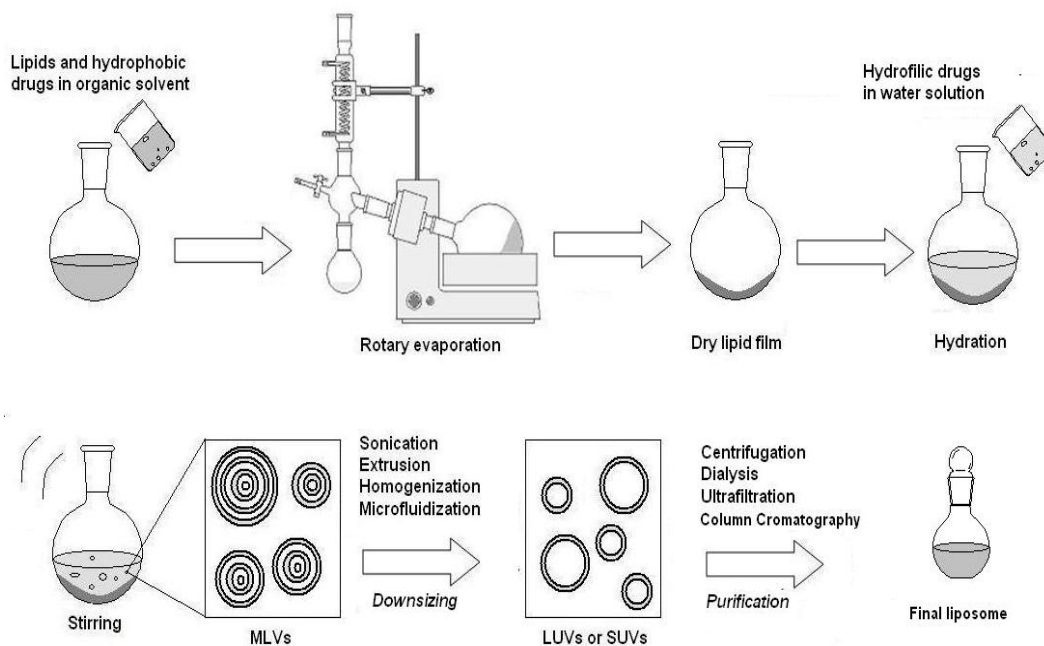


Figure 11: Bangham thin-film hydration method (adapted from de Araújo Lopes *et al.*, 2013)

The pH jump method was first described by Hauser and co-workers in 1982 (Hauser and Gains, 1982). These researchers made mention of the rapid formation of liposomes by increasing the pH from approximately 3 to 11. The liposomes solution containing MLVs is broken down into SUVs or LUVs due to the rapid increase of the buffer solution. After this procedure liposomes must still be extruded to produce a heterogeneous mixture of SUVs. This method, however, was further modified by

Genç and co-workers to produce a homogenous mixture of SUVs compared to the previous heterogeneous mixture (Genç *et al.*, 2009).

2.2.6 Application of liposomes

Since the advent of the discovery of liposomes, they have been used for various applications such as: drug delivery, diagnostics and theranostic uses. Liposomes are mainly used to increase therapeutic effects of existing drug molecules that are toxic to normal tissue. These drugs are encapsulated in either the hydrophobic, lipid-bilayer or hydrophilic, aqueous core, depending on the nature of the molecule. Other applications of liposomes that are being explored are gene delivery, vaccines, respiratory drug delivery, topical applications, etc. Liposomes are currently being used in conjunction with chemotherapeutic agents such as: doxorubicin and its derivatives as first line therapy in breast cancers (Leonard *et al.*, 2009). An example of a commercialised product is Myocet[®] which contains a liposomal mixture of egg phosphatidylcholine (EPC) and cholesterol with doxorubicin as the encapsulated molecule. The studies carried out have shown that Myocet[®] is less toxic compared to free doxorubicin when administered *in vivo* (Kanter *et al.*, 1992). Zhang and co-workers have studied the use of biotinylated-liposomes for the enhancement of insulin delivery via the oral route (Zhang *et al.*, 2014). Biotinylation was achieved via the incorporation of biotin attached to phospholipids into the liposomes. These liposomes produced a significant hypoglycaemic effect and increased its bioavailability compared to conventional liposomes in the blood levels of treated rats. This study has shown to prove the advantage of biotinylated liposomes as a nanocarrier for insulin.

Liposomes also have the ability to be used as nanocarriers for diagnostic applications such as magnetic resonance imaging (MRI), computed tomography (CT), and ultra-sonography (Elbayoumi and Torchilin, 2010). In CT imaging, contrast agents such as iopromide (iodinated organic compounds) are incorporated into the liposomes aqueous core or lipid bilayer (Sachse *et al.*, 1993). Contrast agents, just like any other molecule that is introduced into the body, is rapidly eliminated by the body's RES, thus the need to encapsulate these agents for improved imaging results. Therefore, a lot of research has been conducted on these agents with liposomes and have proven to be successful. However, the main concern regarding these encapsulated agents is the reproducibility on a large scale and making them pyrogen-free and sterile (Tilcock, 1999). A phase 1 clinical trial has been conducted by Høglund and co-workers using liposomes containing iodixanol on 47 healthy volunteers (Leander *et al.*, 2001). The outcome of the study proved to be successful as the researchers found an augmented efficacy of the iodixanol liposomes in the detection of hepatic and splenic tissues and in the early detection of abdominal vesicles.

Although vaccines are currently being used extensively, there are still issues regarding their immunogenicity and stability, and they require numerous administrations. These shortcomings can be overcome by incorporating liposomes into the improvement of vaccines (Kim *et al.*, 2014). Liposomes as adjuvants in vaccines were first mentioned by researchers Allison and Gregoriadis (Allison and Gregoriadis, 1974). The study highlighted the use of negatively charged liposomes that acted as an adjuvant for vaccines against diphtheria toxoids. Properties of liposomes such as: size, lipid composition and structure are parameters that can be

manipulated in order to accommodate different types of vaccine antigens to increase their effects and immunogenicity. Therefore, the surface of liposomes can easily be modified to assist in direct targeting of immune cells to deliver encapsulated molecules such as immunostimulatory agents, and enhance both humoral and cell-mediated immune responses (Kim *et al.*, 2014). These modifications and advancements prove to be advantageous and intensify the efficacy of liposomal vaccines.

2.2.7 Interaction of liposomes with cells

Liposomes are used to deliver drugs intracellularly via basic mechanisms such as endocytosis, diffusion or fusion with cell membranes. Figure 12 is a representation of the mechanisms by which these processes occur. In Figure 12a, liposomes can be specific for receptors on cell membranes or be non-specific (Figure 12b) and be taken up into cells to deliver drugs intracellularly. Figure 12c depicts the fusion mechanism that certain phospholipid-containing liposomes obtain; they destabilise the liposome membrane allowing it to fuse with the cell membrane and thus deliver a payload of drugs intracellularly. Figure 12d shows the ability of liposomes to release their encapsulated drug molecules outside the cell membrane thus allowing the molecules to diffuse into the cells via a concentration gradient. Liposomes may also be subjected to endocytosis (Figure 12e) which can be receptor-mediated or non-specific.

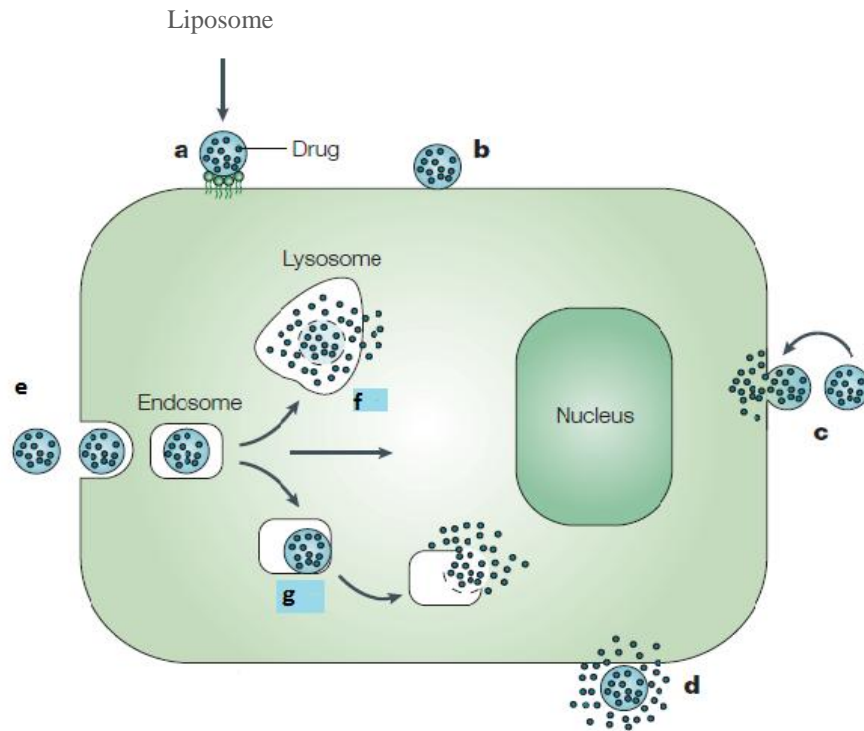


Figure 12: Schematic representation of intracellular delivery of liposomes in cells (adapted from Torchilin, 2005)

2.2.8 Liposomes in drug delivery

Passive targeting is the ability of non-targeted liposomes to utilise the leaky vasculature of blood vessels that supply the tumour to enter the tumour sites via the enhanced permeability and retention effect (EPR). The EPR effect allows for liposomes to be accumulated significantly at diseased tissues such as tumour sites rather than at normal tissue sites which presents an advantage for the delivery of drug molecules intended for the management of cancer.

Active targeting is opposite to passive targeting where there is an antibody that is specific for an antigen expressed in the tumour cell. These specific antibodies can be attached to liposomes containing encapsulated drug molecules and can be delivered into the tumour cell via receptor mediated endocytosis. Active targeting is a lot more

complex compared to passive targeting in a manner that specific antibodies would have to be conjugated onto the surface of liposomes for the tumour cell of interest. Targeting liposomes with encapsulated drug molecules have the ability to treat tumours that are explicitly targeted with conjugated ligands, while non-targeting liposomes have the capability to treat a broader range of tumours due to the liposomes not being specific, taking into account that the drug molecule has a broad spectrum of anti-tumour activity.

In summary, the aim of this study is to prepare an optimal liposome preparation that has the capabilities and characteristics of passive targeting. The research project aimed to formulate a liposome preparation that has fusogenic properties that will have the ability to fuse with the membranes upon contact with the tumour cell lines. Such liposomes will have the ability to deliver payloads of drugs directly into the diseased cells without great costs of active targeting and binding of antibodies onto liposomes.

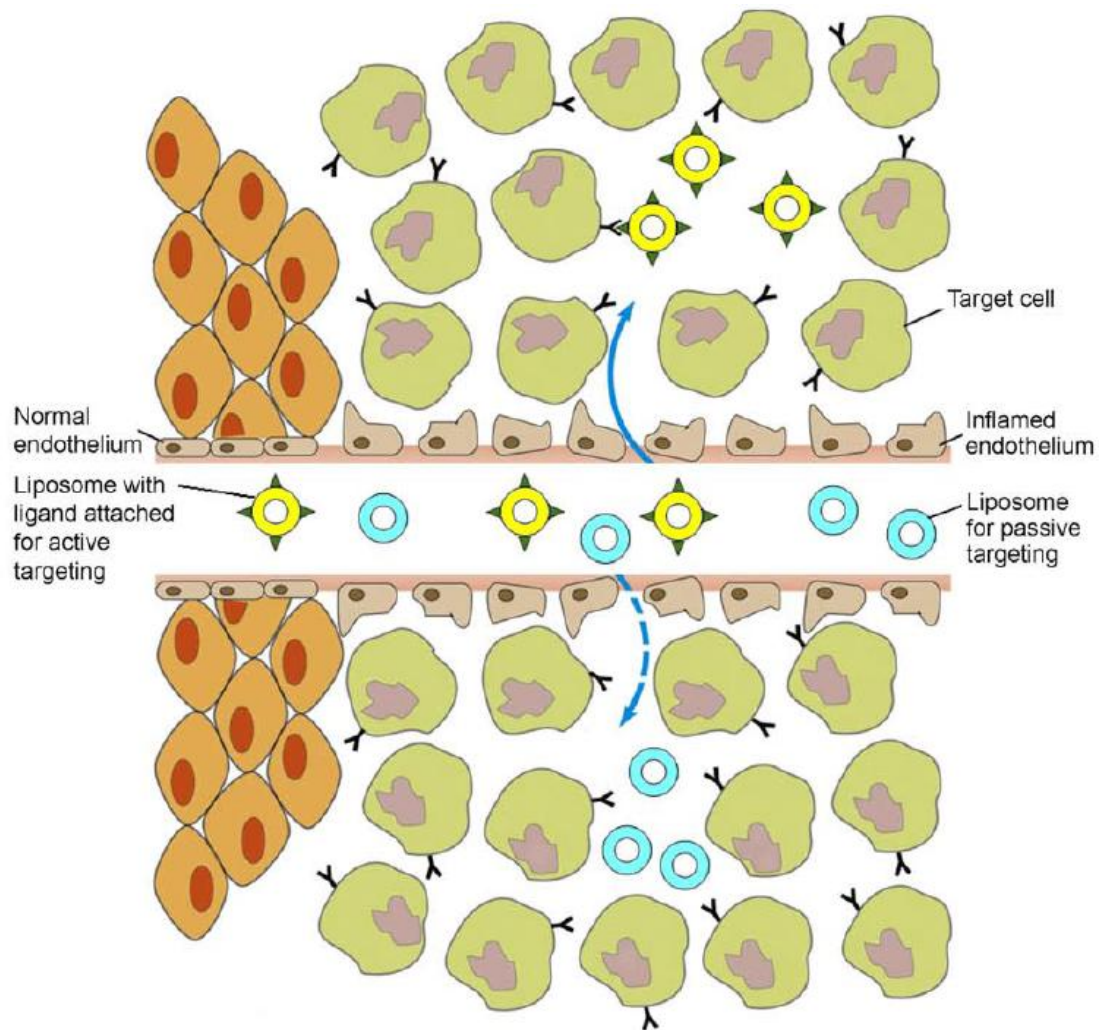


Figure 13: The above figure represents the pathways taken by liposomes via active targeting and passive targeting (adapted from Ghosh *et al.*, 2008)

2.3 Cell culture models

2.3.1 The use of Cell culture models

Research with malignant cell culture was initially carried out by researchers Carrel and Burrows in 1911 in which they have successfully grown chicken sarcoma outside the body. Attempts were made to grow human carcinoma but failed as the cells were endangered by the rapid process of liquefaction (Carrel and Burrows, 1911). Thereafter, an immortal cancer line, HeLa, was first isolated from a Caucasian woman named Henrietta Lacks in 1951 (Scherer, et al., 1953). Cell culture models have been extensively used in cancer research, as they are easy to establish and highly reproducible.

The most common cancer cell model used in primary cancer research is the two-dimensional model which consists of a monolayer of cells grown on plastic petri-dishes supplemented with specific cell culture medium. Two-dimensional cancer cell models have the advantage of controllable conditions, reproducibility, sensitivity, homogeneity and sustainability (van Marion *et al.*, 2015). These advantages allow cancer models to be used in basic cancer research as well as to prove hypothesis. For the purpose of this study three cancer cell lines were used utilising a two-dimensional approach. These cell lines include MCF-7, Caco-2 and C3A cancer cells and their characteristics are discussed below.

2.3.2 MCF-7 cell line

The first human breast carcinoma cell line known as BT-20 was isolated by researchers Lasfargues and Ozzello in 1958 (Cailleau, et al., 1978). Thereafter,

almost 20 years later, a series of breast carcinoma cell lines were established with MCF-7 being the most commonly used worldwide due its overexpression of the estrogen receptor (ER) making it an ideal candidate for hormone receptor studies (Holliday and Speirs, 2011). Current anti-cancer treatment used for breast cancer has shown to have some degree of resistance to the ERs resulting in over expression of ERs and ultimately enhancing tumour growth (Levenson & Jordan, 1997). Hence, this results in the need for new drug discoveries in treatment of breast carcinomas. For the purpose of the study MCF-7 cell line was chosen in order to design an optimal liposomal drug delivery system that utilises a non-targeted approach for anti-cancer therapies.

2.3.3 Caco-2 cell line

In the early 1970's a series of gastrointestinal (GI) tumour cells were isolated for the purpose of cancer research of which a decade later the Caco-2 (colon adenocarcinoma) cell line became the most favoured in GI cancer studies. Early studies on Caco-2 cell lines have shown that these cell lines mimic the morphological and biochemical characteristics of normal intestinal enterocytes (Sambuy et al., 2005). The Caco-2 cell line is also highly attracted by researchers due to their association between intracellular glycogen levels and high growth rate. Another distinctive feature of Caco-2 cells is their ability to express several brush border enzymes which makes them a good model for differentiated enterocytes *in vitro* (Quaroni and Hochman, 1996). Taking into account the similarities observed in normal intestinal tissue and Caco-2 cell lines, researchers that advantage of these characteristics in drug absorption studies and cancer research. Therefore, for the purpose of this study, Caco-2 cell lines will be used in order to represent normal

intestinal tissue and the criteria used for the optimal batch in the statistical design model would we to minimise liposomal uptake into the cell line in order to reduce GI side effects.

2.3.4 C3A hepatocytes cell line

The C3A cell line is a derivative of HepG2, both of which are derived from hepatocellular carcinomas. Hepatocellular carcinomas are the primary cancer of the liver and although major advancements in treatments and diagnostics it is reported that patients die after 1 year of diagnosis which is highly contributed to resistance to therapy (Zhang et al., 2015). The liver is characteristically a site where drug metabolism occurs rapidly which could mainly explain the need for new and improved treatment approaches for hepatocellular carcinomas. An ideal approach for treatment of hepatocellular carcinomas would be to deliver a payload of anti-cancer drug molecules directly into the hepatocellular carcinoma in order to avoid the characteristic of rapid metabolism.

Chapter 3: Methodology

3.1 Materials

Phosphatidylserine (PS), 1,2-dioleoyl-*sn*-glycero-3-phosphoethanolamine (DOPE), cholesteryl hemisuccinate (CHEMS), 1,2-dimyristoyl-*sn*-glycero-3-phosphoethanolamine-N-[methoxy(polyethylene glycol)-2000] (ammonium salt) (PEG₂₀₀₀-PE) and 1,2-dioleoyl-*sn*-glycero-3-phosphoethanolamine-N-(carboxyfluorescein) (PE-CF) was purchased from Avanti Lipids (Alabaster, USA). GIBCO® RPMI Media 1640, Dulbecco's Modified Eagle Medium (DMEM), HyClone™ trypsin 0.25 % and HyClone™ Fetal Bovine Serum (U.S) was purchased from Thermo Scientific. Phosphate Buffered Saline (PBS Buffer; pH 7.4).

3.2 Liposome preparation

Liposomes with different lipid compositions were prepared using the thin-film hydration method (Koshkaryev et al., 2013, Evjen et al., 2010). In brief, 40 mM of the specific lipid formulations, as described in Table 3, were completely dissolved in a 5 ml chloroform:methanol mixture (9:1 v/v) and rotary evaporated (Büchi Labortechnik AG, Flawil, Switzerland) at 50 °C under vacuum for three hours until dry. The remaining solvent was removed by flushing the film with nitrogen. The dried lipid film was then stored at -20 °C prior to use. PE-CF was added to the lipid preparations in order to visualize the liposomes under fluorescent microscopy and for flow cytometric analysis.

The resulting dried lipid films were hydrated with 5 ml of pre-heated PBS buffer (pH 7.4) in a shaking hot water bath at 60 °C for three hours. Prior to extrusion, filter membranes were wetted by extruding deionised water 11 times. The resulting multilamellar liposome vesicles were then extruded 15 times through a 100 or 200 nm (according to the experimental design) pore size polycarbonate filter (Nuclepore) using a mini-extruder (Avanti Polar Lipids, Alabaster, USA). The small unilamellar vesicles (SUV) formed were stored at 4 °C prior to use.

Table 3: Representation of the quantity (mg) of lipid compositions used in preparing batches 1-8 and the optimal batch.

	Liposome preparations								
Batch	1	2	3	4	5	6	7	8	Optimal
PS	19.63	28.37	18.48	-	-	-	29.53	-	21.73
DOPE	-	-	-	25.60	26.64	17.71	-	16.67	-
CHEMS	7.78	1.95	7.78	1.95	1.95	7.78	1.95	7.78	4.49
PEG ₂₀₀ -PE	0.54	4.31	4.31	4.31	0.54	0.54	0.54	4.31	4.31
PE-CF (1%)	0.28	0.35	0.31	0.32	0.30	0.26	0.32	0.29	0.30
Liposome size (nm)	200	200	100	100	200	100	100	200	200

3.2.1 Experimental design

With regards to the experimental design used in the study, a design protocol was developed using a conventional two-level factorial design. The design was created utilising Design-Expert® software (Stat-Ease, Inc., Minneapolis, USA) (Whitcomb, P, 2015). The primary screening design was conducted using a 2⁴⁻¹ fractional factorial design that took into account the four parameters that were used to determine the optimisation of the liposomal preparation. This design was used in order to minimise

the number of experimental runs as the aim of the study was to determine the ranges of the parameters that were furthestmost optimal in formulating an ideal liposome preparation for fusion with tumour cell line membranes.

As part of the objectives of the study, a thorough search of the literature was performed in order to pinpoint which parameters would need to be included into the study design in order to manipulate an optimised liposome preparation. The parameters that were identified were: Type of phospholipid (either phosphatidylserine (PS) or phosphoethanolamine (DOPE)), concentration of cholesteryl hemisuccinate (CHEMS), concentration of poly (ethylene glycol) (PEG₂₀₀₀)-phosphatidylethanolamine (PE) and the size of the liposome, either 200 nm or 100 nm as shown in Table 4.

Code[Type]	Parameter	Units	Low level	High level
A[categorical]	Phospholipid type	-	PS	DOPE
B[numerical]	[CHEMS]	mM	10 %	40 %
C[numerical]	[PEG ₂₀₀ -PE]	mM	0.5 %	4 %
D[categorical]	Liposome size	nm	100	200

As a result of the design, eight experimental runs were produced and were carried out in triplicate on the three cell lines in order to increase the statistical power of the design. Table 5, below, outlines the full experimental runs in randomised order. The study was performed in two parts in which the first part was to synthesise 8

experimental batches which would determine the optimal parameters to be used in the second part of the study which was to synthesise an optimal liposome preparation. The validation of the 8 batches was carried out through the preparation of the liposomal formulations set out by the statistical design model and tested on the three tumour cell lines. Thereafter, the criteria used for determining the optimal liposome batch was by maximising liposomal uptake into MCF-7 and C3A cell lines and minimising uptake into Caco-2 cell lines as this cell line is a representative normal gastrointestinal tissue.

Table 5: Experimental runs for primary screening of optimal liposome preparation using 2⁴⁻¹ fractional factorial design						
Experiment	Sequence (Batch No.)	Factors				
		PS (%)	DOPE (%)	CHEMS (%)	PEG ₂₀₀ -PE (%)	Liposome size (nm)
5	1	86	-	10	4	200
8	2	-	56	40	4	200
1	3	89.5	-	10	0.5	100
7	4	56	-	40	4	100
2	5	-	89.5	10	0.5	200
6	6	-	86	10	4	100
3	7	59.5	-	40	0.5	100
4	8	-	59.5	40	0.5	200

3.3 Liposome characterisation

3.3.1 Zeta potential and particle size analysis

Particle size, polydispersity and zeta potential of the liposomes were measured using photon correlation spectroscopy (PCS) using a Malvern Zetasizer™ Nano ZS particle size analyser (Malvern Instruments Ltd., Malvern, UK). Photon correlation spectroscopy, also known as dynamic light scattering, is the only technique able to measure particles in a solution or dispersion in a fast, routine manner with little or no sample preparation. Photon Correlation Spectroscopy has the advantages of small measurement times, typically in seconds or at most a few minutes, with the sample having been through the minimum of preparation. Preparation of samples by other techniques will change the characteristics of the liposomes like agglomeration, etc. The PCS measurements were carried out at a scattering angle of 90°. The samples were diluted at 1:9 (v/v) in distilled water and filtered with a 23 mm, 0.22 µm membrane filter to avoid multi scattering phenomena and placed into a clear folded capillary cell. Samples were measured at 25 °C and in triplicate. For particle size, the instrument was set to automatically determine attenuator level measurement position and number of sub-runs based on correlation data. For zeta potential measurements, the attenuator setting and number of sub-runs was automatically determined by the instruments according to phase plot data.

3.3.2 Atomic force microscopy (AFM)

Atomic force microscopy was performed on the optimal liposome to visualise the shape and size of the drug delivery vesicle. Mica sheets were chosen as a solid substrate and used immediately after cleavage in a clean atmosphere. Basically, a drop of liposome preparation was placed onto the surface of freshly cleaved mica

which was then left to dry at room temperature. After approximately 20 minutes the prepared mica sheets containing the dried liposome preparation were then transferred to a Bruker® AFM for imaging. The scans were performed in air with a Fast-scan equipped with ScanAsyst. A silicon tip, with a diameter of \approx 5-10 nm, on a nitride lever (Si_3N_4) was used to scan the liposomal preparations. The images and diameter of the captured liposomes were analysed utilising NanoScope Analysis (Bruker®) software.

3.4 Cell culturing

MCF-7, Caco-2 and C3A cells available at the Department of Biochemistry and Microbiology (NMMU) were maintained in their respective media (as described below) in an atmosphere comprising 95% air supplemented with 5% CO_2 at 37 °C.

3.4.1 Handling procedure for frozen cells

Frozen vials containing cell cultures were thawed by gentle agitation in a 37 °C water bath (approximately two minutes). Vials were removed from the water bath as soon as the contents were thawed, and decontaminated by spraying with 70 % ethanol. The contents of the vial were transferred to a centrifuge tube containing 9.0 ml complete culture medium in a laminar flow hood and spun at approximately 1250 rpm for five minutes. All of the operations from this point on were carried out under sterile conditions. The supernatant was discarded by aspiration using a Pasteur pipette. The pellet was re-suspended with the complete cell culture medium and dispensed into a 60 mm cell culture dish. Prior to the addition of the vial contents, the culture vessel containing the complete growth medium was placed into the incubator

for at least 15 minutes to allow the medium to reach its normal pH (7.0 to 7.6). The cultured cell was incubated at 37 °C in an incubator with 5 % CO₂.

3.4.2 Cell growth medium

The MCF-7 cell line was maintained in Roswell Park Memorial Institute (RPMI)-1640 medium. The Caco-2 cell line was maintained in Dulbecco's Modified Eagle's medium (DMEM). The C3A cell line was maintained in Eagle's minimal essential medium (EMEM) supplemented with 1 % Non-Essential Amino Acid (NEAA). All cell lines were supplemented with 10 % Foetal Bovine Serum (FBS) cultured in 60 mm cell culture dishes and incubated at 37 °C with 5 % CO₂.

3.4.3 Sub-culturing

Sub-culturing was done when cells were 80 % confluent. The culture medium was removed using a sterile Pasteur pipette and aspirator. The plate was washed twice with 10 ml of sterile phosphate buffered saline (PBS), pH 7.4. Then, 1 ml of Trypsin/EDTA solution was added to the cell culture dish and observed cells under an inverted microscope until cell layer was dispersed (usually within 5 to 15 minutes). Cells were then counted using a haemocytometer and appropriate aliquots of the cell suspension was added to new culture dishes. Thereafter, 9 ml of complete growth medium was added to cell culture dishes and disperse cells by gently pipetting.

3.5 Intracellular delivery of liposomes

3.5.1 Fluorescence microscopy

After an initial passage in cell culture dishes, MCF-7, Caco2 and C3A cells were grown in 12-well cell culture plates at a seeding density of 150 000 cells/well. After reaching 70-80 % confluence, the plates were washed twice with 1 ml PBS (pH 7.4). The cells were then treated with 100 μ L of the specific liposome preparation. Thereafter, 900 μ L of serum-free culture medium was pipetted into each well and then incubated for 1 h at 37 °C. The plates with cell controls were washed twice with 1 ml PBS (pH 7.4) and 1 ml serum-free cell culture media was pipetted into the wells and incubated as above. After incubation the cells were washed twice with 1 ml PBS (pH 7.4). Cells were observed with a Zeiss inverted fluorescence microscope under bright light or fluorescence with green filter (excitation/emission: 485/512).

3.5.2 Flow cytometry analysis

Intracellular uptake of liposomes in cells was determined by flow cytometry assay. MCF-7, Caco 2 and C3A cells were grown in 12-well cell culture plates at a seeding density of 150 000 cells/well and incubated for 24-48 hours at 37 °C and 5 % CO₂. After reaching 70-80 % confluence, the plates were washed twice with 1 ml PBS (pH 7.4). 100 μ L of each liposome formulation was added to the cells and incubated for one hour at 37 °C in a 5 % CO₂ incubator in an appropriate serum-free culture medium. Thereafter, each well was washed twice with 1 ml PBS (pH 7.4) and 100 μ L of 0.25 % of trypsin was added to each well. Cells were incubated for approximately five minutes until cell detachment. 900 μ L of complete cell culture medium was added to each well and pipetted into 4 ml flow cytometry tubes. Cells were then

pelleted by centrifugation at 1800 rpm for five minutes. Cells were washed twice with 1 ml PBS (pH 7.4) and centrifuged after each step. Thereafter, 0.3 ml of PBS was added to the cells and placed on ice. Within 30 minutes the cellular uptake of liposomes was analyzed using flow cytometry (FACS) by using a Becton-Dickinson FACScan. Data was collected at 10,000 gated events and analyzed with the CELL Analysis software (Becton-Dickinson Immunocytometry System, Mountain View, CA).

3.6 Statistical Methods

All experiments were conducted in at least triplicate and the results reported descriptively as means +/- standard deviation. ANOVA analysis was used in the experimental design to fit the data generated to the mathematical models proposed. A probability (p) value was calculated to distinguish significance within the 95% confidence interval where $p < .05$ was defined as significant.

Chapter 4: Results and discussion

4.1 Batch optimisation experiments

4.1.1 Characterisation of liposomes

4.1.1.1 Photon correlation spectroscopy

The particle size and zeta potential analysis was performed on a Zetasizer™ using photon correlation spectroscopy. The results are shown in Table 6 below. The range of the liposomes was from 78.9 to 167.6 nm for both 100 and 200 nm filtered liposomes. Batches 1, 5 & 8 had an average value of 125.2, 158.7 & 167.6 nm respectively with a standard deviation of ± 1.02 , 1.90 & 1.75 respectively indicating a good variation in the particle size of the batches. Batch 2 had an average value of 98.1 nm with a standard deviation of ± 0.86 . The results from batches 1, 2, 5 & 8 indicate that the extrusion method using 200 nm polycarbonate membrane filters employed to size the liposomes to 200 nm is adequate and produces liposomes with a good variation in particle size. Batches 3, 4, 6 & 7 were extruded in the same manner, but instead a 100 nm polycarbonate membrane filter was used as per the experimental design. Batch preparations 3 & 7 produced average particle sizes of 78.9 and 93.5 nm with standard deviations of ± 0.45 and 1.00, respectively, thus indicating a good variation in the particle size analysis. However, batch preparations 4 & 6 produced average particle sizes of 120.4 and 124.5 with standard deviations of ± 1.93 and 1.03, respectively. The length of time between extrusion and PCS analysis was almost immediately. Therefore, the size of the liposomes which were observed to be > 100 nm could be due to their flexibility and ability of the large liposomes to squeeze through the pore size of the membrane (MacDonald *et al.*,

1991). However, the variation in the particle size is good, which is an indication that the extrusion method worked as soundly as was anticipated.

Liposomes prepared with phospholipid, DOPE, can be seen to play an important role in the variable particle sizes of both liposomes extruded through 100 and 200 nm membranes, specifically batches 2, 6 & 8. Batch 2 has a low concentration of DOPE present but a high concentration of PEG which could indicate that small liposome vesicles were formed by the thin-film hydration method and were sterically stabilized so as to avoid fusion between liposome vesicles, hence keeping the liposome vesicles at particle sizes of <100 nm. Batches 4 and 6 could have produced larger liposome particle sizes due to fusion of smaller sized vesicles after the extrusion process with the 100 nm polycarbonate membrane filter.

Table 6: Representation of particle size, polydispersity index and zeta potential of experimental design batches 1-8			
Batch No.	Average particle size (nm)	Average polydispersity index (PI)*	Average zeta potential (mV)
1	125.2 (±1.02)	0.174 (±0.009)	-67.44 (±2.90)
2	98.1 (±0.86)	0.175 (±0.009)	-29.10 (±1.63)
3	78.9 (±0.45)	0.140 (±0.020)	-22.83 (±0.68)
4	120.4 (±1.93)	0.101 (±0.012)	-26.48 (±0.82)
5	158.7 (±1.90)	0.170 (±0.016)	-47.05 (±1.58)
6	124.5 (±1.03)	0.086 (±0.015)	-53.82 (±1.82)
7	93.5 (±1.00)	0.120 (±0.010)	-58.30 (±2.00)
8	167.6 (±1.75)	0.166 (±0.011)	-33.40 (±1.55)

*PI represents the polydispersity index used as indication of size distribution of vesicles.

4.1.2 Intracellular delivery of liposomes

4.1.2.1 Flow cytometry analysis

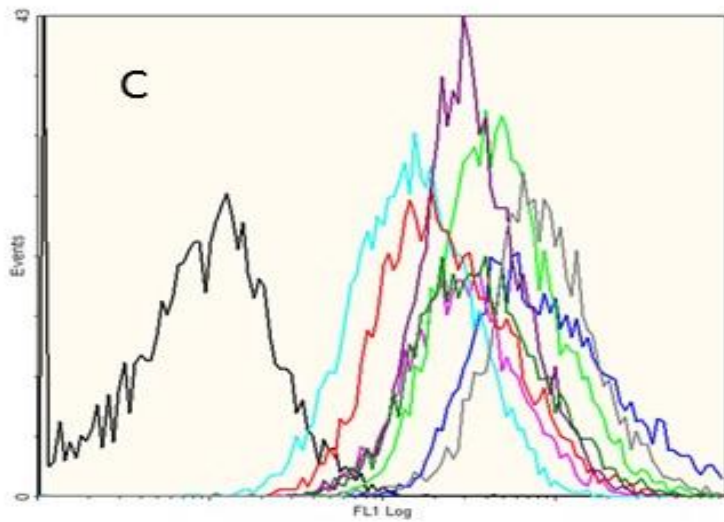
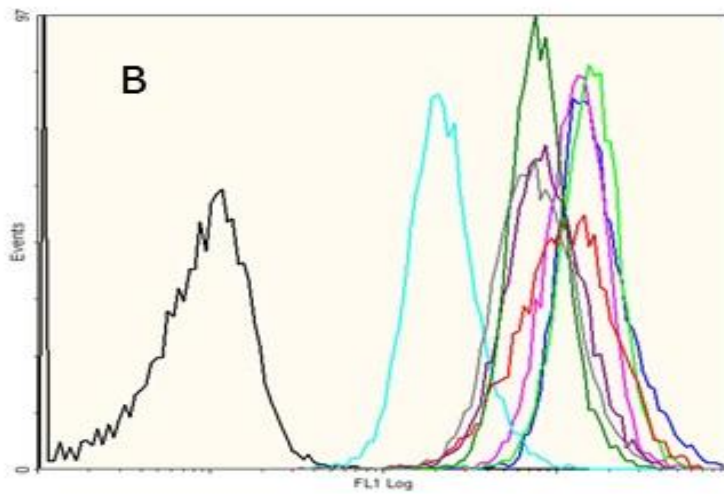
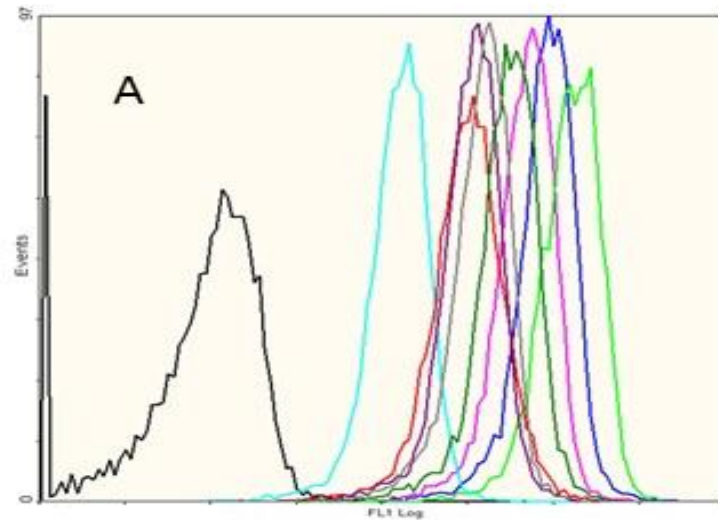
4.1.2.1.1 Uptake into cell lines

Flow cytometry analysis was carried out in order to determine the amount of liposome that was taken up into the tumour cells using 1,2-dioleoyl-sn-glycero-3-phosphoethanolamine-N-(carboxyfluorescein)(PE-CF) (PE-CF) as a fluorescent marker. Table 7 below is a representation of the flow cytometry results indicating the uptake and amount of liposomes taken up into cells when exposed to the liposomal batches 1-8. Flow cytometry work was carried out on MCF-7, Caco-2 and C3A tumour cell lines. The experiments were carried out in triplicate. The averages of the mean fluorescence intensities were calculated for each batch on each cell line. The results of these experiments were employed into the statistical design in order to determine and calculate the optimised batch. To have a better understanding of the uptake of the liposomes into the cell lines, an overlay plot was drawn. The overlay plots in Figure 14 clearly indicate the shift of the graphs to the right from the control (black- untreated cells) for the MCF-7(A), Caco-2(B) and C3A (C) cell lines. The y-axis on the graph indicates the mean fluorescence intensity of each cell line treated with the fluorescent liposome at different compositions while the x-axis is an indication of the number of events. Batches that are taken up efficiently into the cells are shown to shift more to the right on the graph than batches which have not been taken up efficiently.

The graphs from the MCF-7 and Caco-2 cell lines have shown that these cell lines have been effectively taken up compared to the C3A cell line. The mean values of

the results were calculated for all batches and employed into the statistical design to create an optimised batch for uptake into the same tumour cell lines.

Table 7: Representation of the average mean fluorescence intensity (MFI) results for batches 1-8 in flow cytometry for MCF-7, Caco-2 and C3A cell lines			
Batch No.	Average (AVG) Mean fluorescence Intensity (MFI)		
	MCF-7	Caco-2	C3A
1	98.47	190.50	126
2	94.53	139.83	117.5
3	189.50	173.5	98.40
4	15.63	23.01	42.68
5	30.91	94.5	52.75
6	34.35	94.60	88.18
7	64.40	87.77	109.33
8	41.2	74.40	92.02



Key (A,B & C)	
Colour	Name
Black	Control
Dark blue	Batch 1
Pink	Batch 2
Neon green	Batch 3
Turquoise	Batch 4
Red	Batch 5
Purple	Batch 6
Dark green	Batch 7
Grey	Batch 8

Figure 14: Overlay plots of the flow cytometry results for batches 1-8 performed on A: MCF-7, B: Caco-2 and C: C3A with the x-axis being the number of event and y-axis being the Mean fluorescence intensity (FL1 Log)

4.2 Statistical optimisation

Once the lipid compositional factors appropriate for fusion with tumour cell line membranes were identified from literature, Design-Expert® (Stat-Ease, 2015) was used to derive the 8 experimental formulations as described previously. The experimental preparations were formulated and subjected to the tumour cell lines for flow cytometry analysis. Thereafter, the MFI results were utilised in the statistical software to formulate the optimal liposome preparation. The statistical results of the 8 experimental runs will be further discussed below.

4.2.1 Liposome uptake into MCF-7 cell lines

The ANOVA analysis of the model for the response showed that the Response Surface Reduced 2FI model used for the analysis was significant with an F-value of 2858.03 and a p-value of 0.0143 ($p < 0.05$). Thus, this indicates the model could be used to evaluate the design space. To test how well the model was suited to make predictions, a graph of predicted responses as a function of actual responses was created. As seen in the graph below, Figure 15, the actual values fall close to the predicted design space.

The formulations were tested with regards to their uptake efficiency and the results were analysed to determine which of the variables, either PS or DOPE, or what concentrations of CHEMS and PEG₂₀₀₀-PE and liposome size was optimal. One factor plots of each variable was plotted by the statistical design software in order to indicate the influence the variables had on the uptake of the liposome into the cell lines. The individual graphs can be seen below in Figure 16. The ANOVA analysis for the phospholipid type was calculated to be a p-value of 0.0056. It can be seen

from the graph that the phospholipid type has a distinguished impact on the uptake of the liposomes into the MCF-7 cell line with PS being the most favoured over DOPE. The liposome size had a slight effect on the uptake with a p-value of 0.0486. The liposome size of <100 nm was not perceptibly more significant than the 200 nm indicating that sizes ranging between 100 and 200 nm can be optimal in uptake into MCF-7 cell lines. It can be noted from the graphs of the CHEMS and PEG₂₀₀₀-PE that, with increasing concentration, the liposomal uptake into the MCF-7 cell line increases. The ANOVA analysis for CHEMS was found to be a p-value of 0.0131, which is significant, but for PEG₂₀₀₀-PE the p-value was 0.0535. A p-value greater than 0.05 for PEG₂₀₀₀-PE indicates that the variable had no significant effect on the response. It should be noted, however, that the 95% confidence interval cut-off, where a p-value of greater than .05 is an indication of lack of significance, this is not an absolute and value of 0.0535 is fairly close to significance.

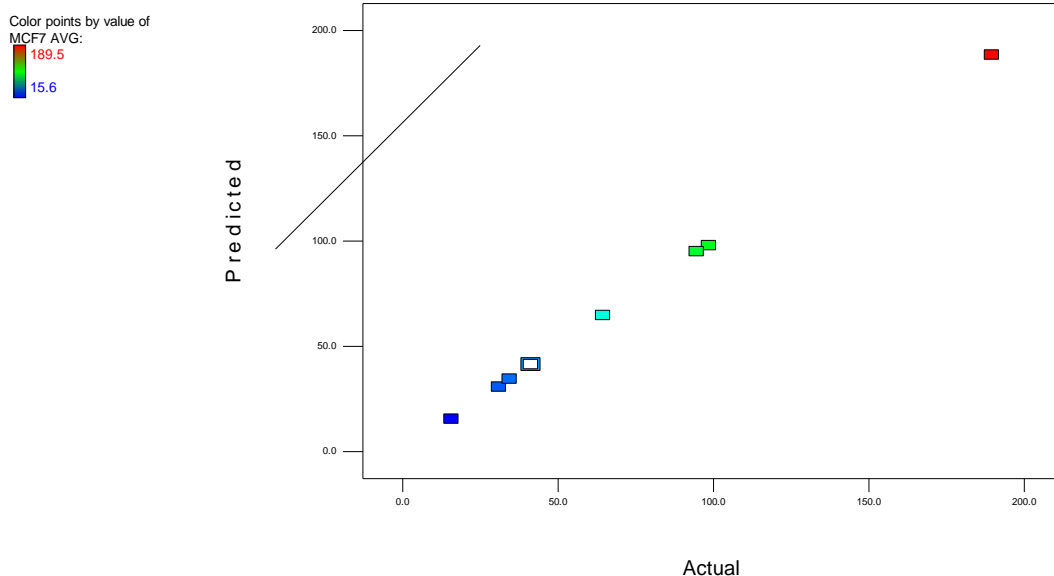


Figure 15: Predicted versus actual results for uptake of liposomes into MCF-7 cell line

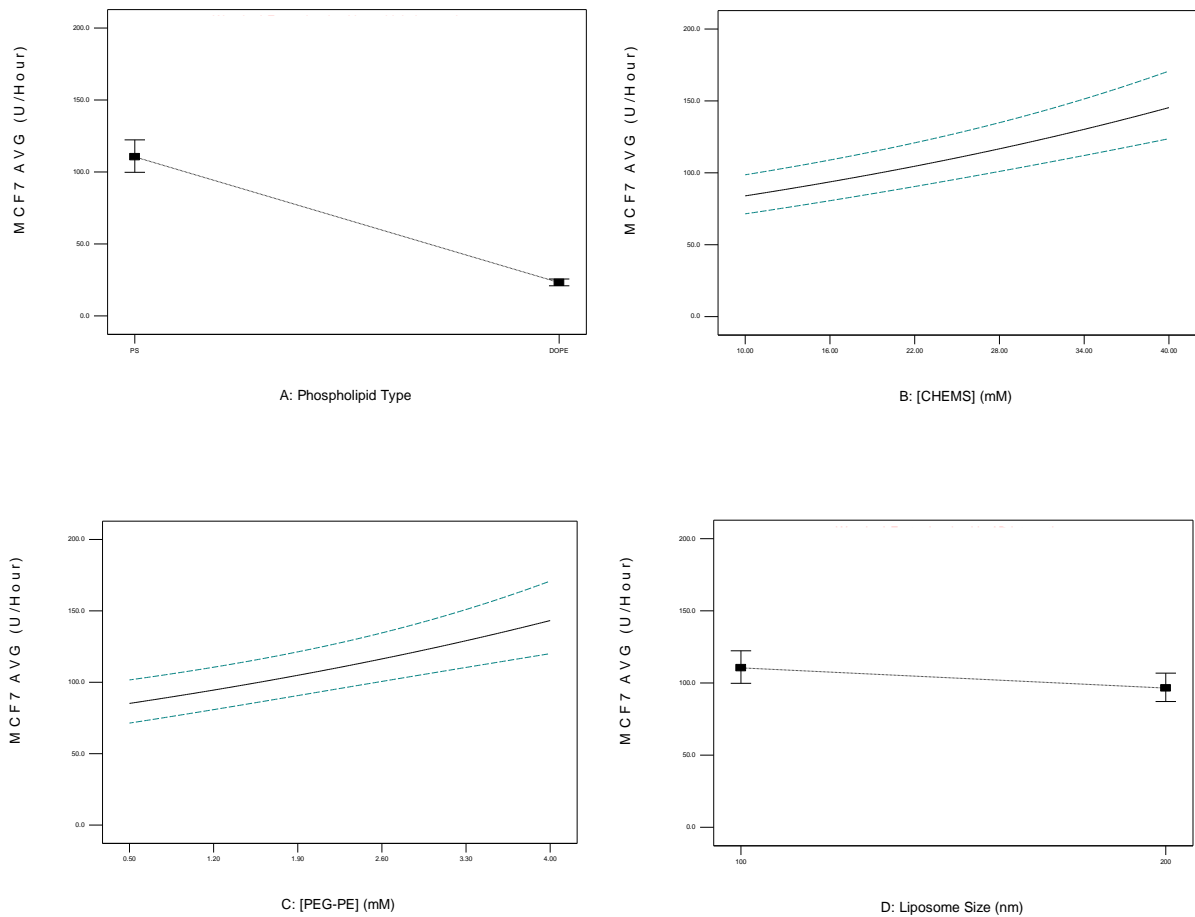
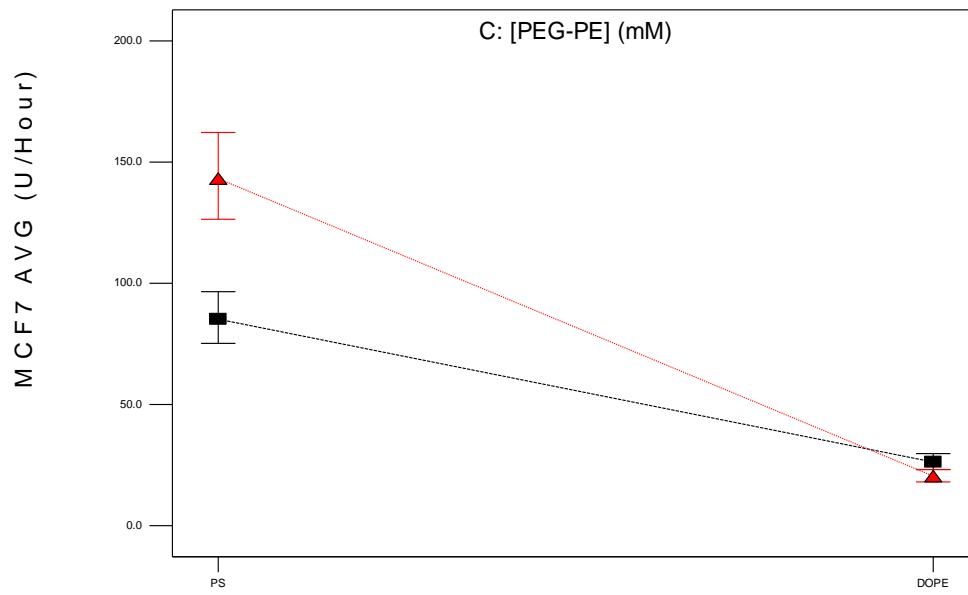


Figure 16: One factor plots for variables in liposomal uptake in MCF-7 cell line

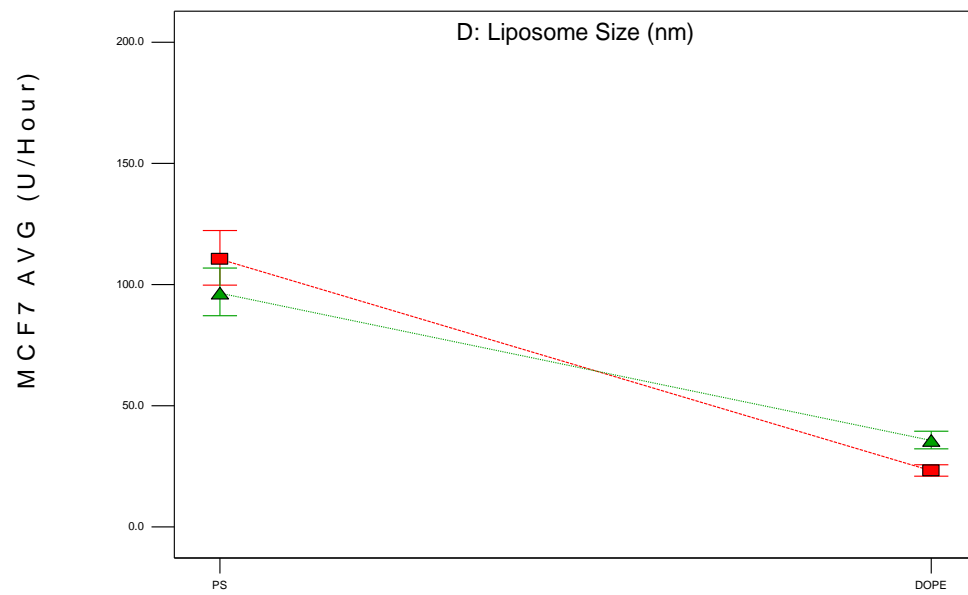
Interactions plots can be used in order to determine which two factors interact with each other within the design space. Figure 17 below represents two graphs that showed interaction between phospholipid type and liposome size or concentration of PEG₂₀₀₀-PE. The most significant interaction was between the phospholipid type and liposome size, where complete convergence of both the lines can be seen to cross each other near the centre of the design space. The ANOVA analysis for the interaction showed a significant p-value of 0.0254. The green dotted line in the graph represents the high level of the variable being the 200 nm liposome size and the red dashed line represents the low level of the liposome size being 100 nm. The 100 nm PS phospholipid liposomes are slightly favourable in uptake compared to the 200 nm

liposomes of the same phospholipid. However, the 200 nm DOPE phospholipid liposomes can be seen to have a higher liposome uptake compared to the 100 nm DOPE phospholipid liposomes. Therefore, high levels of liposomal uptake can be observed with both liposome sizes on the PS phospholipid side compared to the DOPE phospholipid, indicating that PS serves as a favoured variable in liposomal uptake independently of liposome size.

The interaction plot between the concentration of PEG₂₀₀₀-PE and phospholipid type has a significant p-value of 0.0188, indicating that these two variables interact with each other and cannot be manipulated independent of each other. The red line from the graph represents the high level of 4.00 mM concentration and the black line represents the low level of 0.5 mM concentration of PEG₂₀₀₀-PE. High levels of liposomal uptake can be observed with both concentrations of PEG₂₀₀₀-PE with PS compared to that of DOPE phospholipids. This observation is similar with the above interaction mentioned, in which PS is more desirable than DOPE in liposomal uptake in MCF-7 cell lines independently of concentration of PEG₂₀₀₀-PE. It can be predicted from the interaction graph that increasing levels of PEG₂₀₀₀-PE would result in increased uptake making the high level of concentration (4.00 mM) more desired for the batch optimisation of the liposome preparation.



A: Phospholipid Type



A: Phospholipid Type

Figure 17: Interaction plots for variables in MCF-7 liposomal uptake

4.2.2 Liposome uptake into Caco-2 cell lines

Due to Caco-2 cell lines being used in the study as a representative of normal GI tissue, the statistical design model was manipulated in a manner to minimise uptake in order to decrease gastrointestinal side effects. Therefore, the ANOVA analysis of the model for the response showed that the Response Surface Reduced linear model used for the analysis was significant with an F-value of 7.77 and a p-value of 0.0292 ($p < 0.05$). Thus, this indicates the model could be used to evaluate the design space. A graph of predicted responses as a function of actual responses was created. As seen in the graph below, Figure 18, the actual values are shown to be at a 45° angle with values close to the predicted design space.

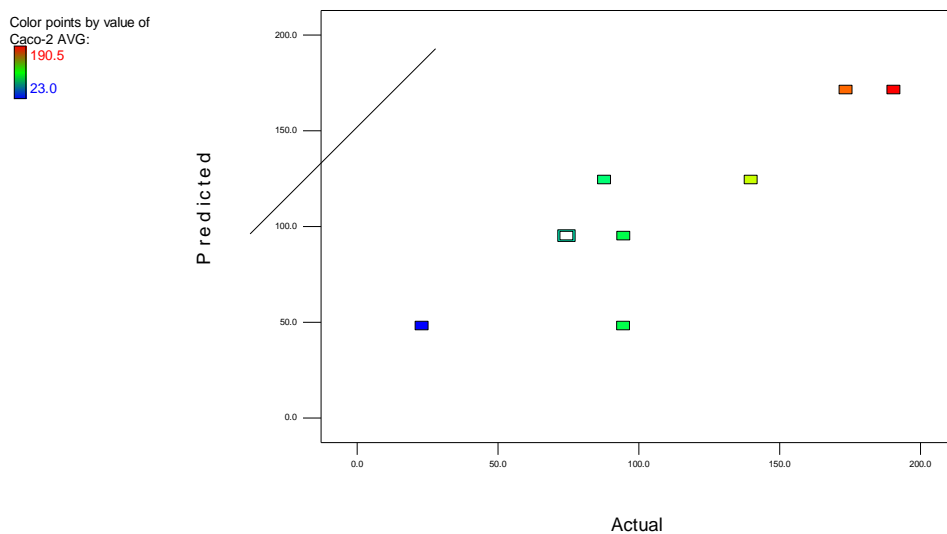


Figure 18: Predicted versus actual results for uptake of liposomes into Caco-2 cell line

As discussed previously, one factor graphs were plotted by the statistical design software in order to indicate the influence each variable had on the uptake of the liposome into the Caco-2 cell lines. The design model chosen by the software to give a significant p-value had excluded two variables, being the liposome size and

concentration of PEG₂₀₀₀-PE as a model reduction was necessary to minimise the statistical noise created by non-significant factors. Phospholipid type and concentration of CHEMS were the only two variables which were found useful in navigating the design space and resulting in a significant model design. The individual graphs can be seen below in Figure 19. The ANOVA analysis for the phospholipid type was calculated to have a significant p-value of 0.0202 while a non-significant p-value of 0.0935 was observed for the concentration of CHEMS. High levels of liposomal uptake can be observed on the PS phospholipid side of the individual plotted graph compared to the DOPE phospholipid, thus indicating that PS, as a phospholipid, is a better component for fusogenic liposomes which can be utilised in the batch optimisation formulation.

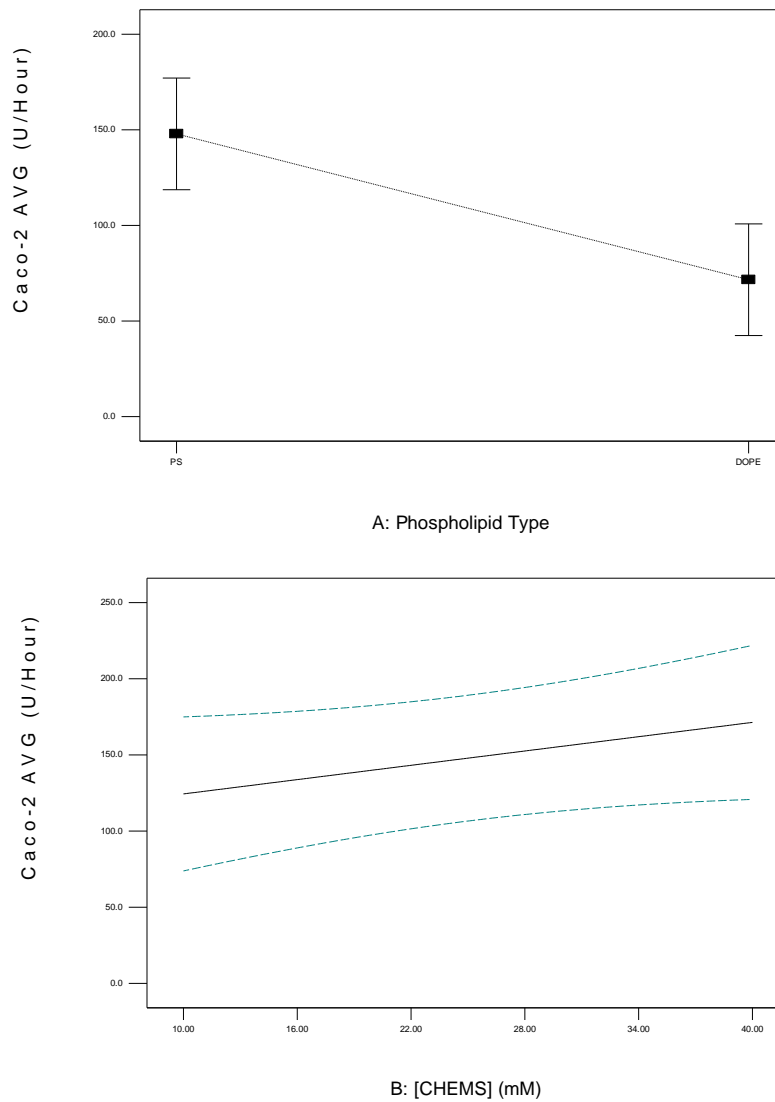


Figure 19: One factor plots for variables in Caco-2 liposomal uptake

4.2.3 Liposome uptake into C3A cell lines

The ANOVA analysis of the model for the response showed that the Response Surface Reduced 2FI model used for the analysis was significant with an F-value of 27.29 and a p-value of 0.0108 ($p < 0.05$). Thus, this indicates the model could be used to evaluate the design space. To test how well the model was suited to make predictions, a graph of predicted responses as a function of actual responses was created, as seen in the graph below, Figure 20, with the actual evaluations falling close to those predicted by the design model.

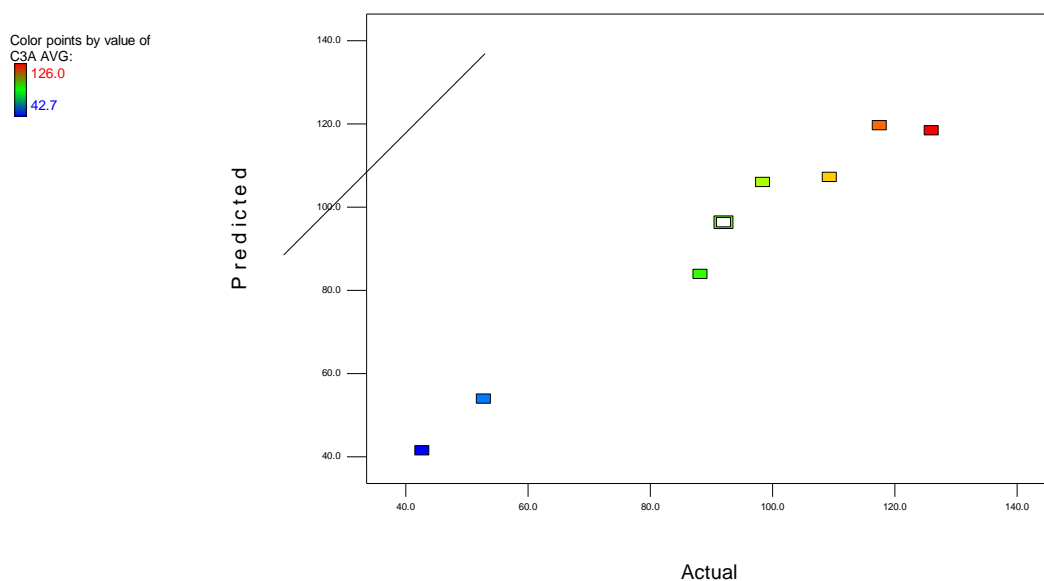
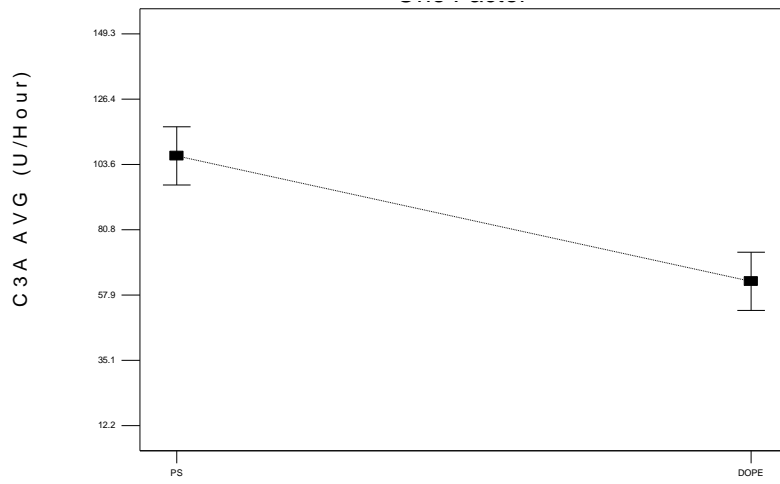


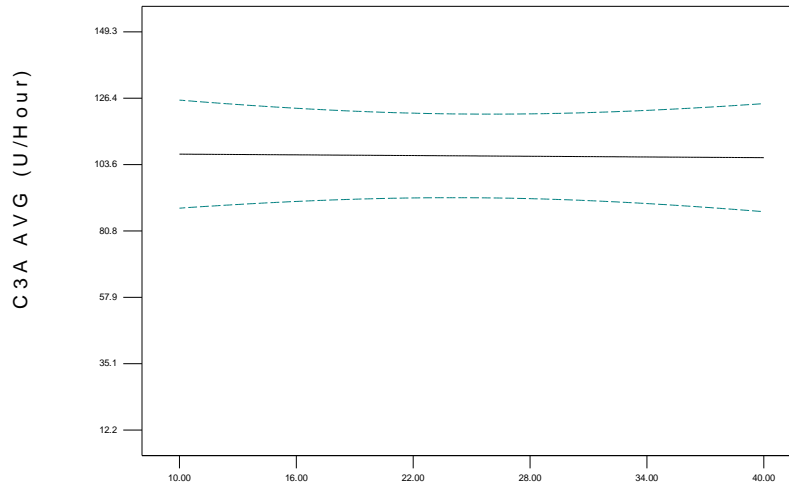
Figure 20: Predicted versus actual results for uptake of liposomes into C3A cell line

One factor graphs were also plotted for the liposomal uptake into the C3A cell lines, shown below in Figure 21. The ANOVA analysis for the variables found the phospholipid type and concentration of CHEMS to be significant with p-values of 0.0035 and 0.0291, respectively. A non-significant p-value of 0.0979 was found for the independent variable, liposome size with a p-value of 0.0979, but was used in order to evaluate the design model which was found to be significant ($p < 0.05$). The phospholipid type graph (Figure 21A) can be seen to have high levels of liposomal uptake observed on the PS side compared to the DOPE phospholipid. This indicates that liposomes consisting of PS are favourable in creating liposomes for optimal uptake into cancer cell lines. The concentration of CHEMS showed to have an almost horizontal line across the graph at a high level of uptake indicating that all concentrations of CHEMS between the studied ranges of 10 to 40 mM can be utilised in preparing optimal liposomes for uptake into C3A cell lines without

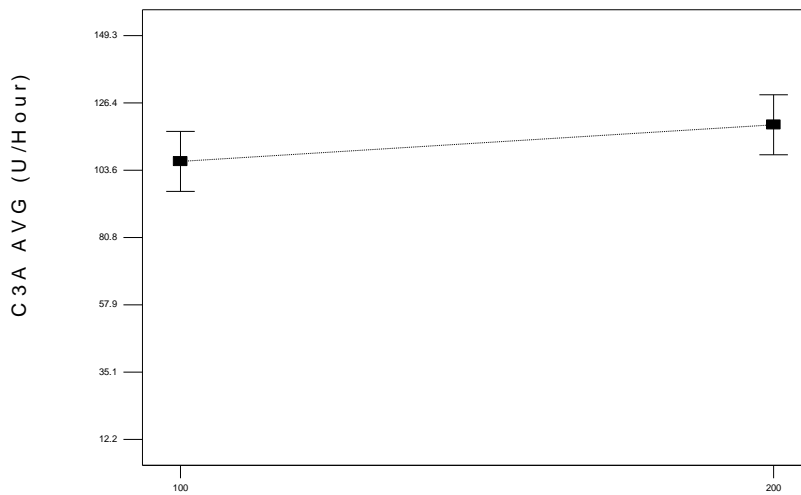
significant differences noted in the response. With regard to the liposome size, 200 nm sized liposomes have shown to have a higher effect on liposomal uptake compared to the 100 nm sized liposomes. This is contrary to the findings of the previous graph of the MCF-7 cell line, where 100 nm were shown to have a higher liposomal uptake into the cell line.



A: Phospholipid Type



B: [CHEMS] (mM)



D: Liposome Size (nm)

Figure 21: One factor plots for variables in C3A liposomal uptake

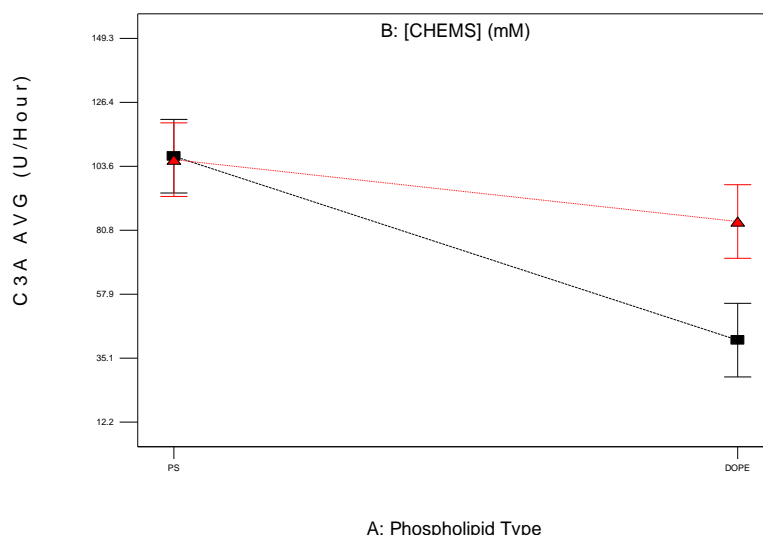


Figure 22: Interaction plot for variables in C3A liposomal uptake

As a result of the experimental runs that were performed on all 8 batches of liposome preparations, an optimised liposomal batch was designed and is shown in Table 8. The criteria that were used to optimise the batch were that the CF flux should be maximised for the MCF7 and C3A tumour cells while minimised for Caco-2 cells as these resembles a number of healthy gastrointestinal tissue's functions.

Table 8: Optimised liposome batch			
Phospholipid Type	[CHEMS] (%)	[PEG ₂₀₀₀ -PE] (%)	Liposome size (nm)
PS	22.91	4	200

The optimised liposome preparation was predicted to have a desirability of 0.634, where the desirability index is a measure of how close each of the predicted responses is to the optimum. The desirability index is therefore a measure of the degree of compromise needed to create a liposome preparation that meets all the required needs for all responses. Based on the flow cytometry results, the most

acceptable phospholipid to be used for the optimised batch is PS and CHEMS for the rigidity of the liposome structure. The percentage of PEG₂₀₀₀-PE did affect the statistical design as the highest concentration amount was chosen to be best suited for the intracellular delivery of the liposomes. The liposome size that had the predicted desirability to be taken up into the tumour cell lines was chosen to be 200 nm.

4.3 Optimised batch characterisation

4.3.1 Liposomal uptake into the MCF-7, Caco-2 and C3A cancer cell lines

The average MFI results obtained from the optimised liposome preparation runs on the three cancer cell lines are shown to be relatively low compared to the predicted mean values proposed by the statistical model. A graph of the actual values compared to the predicted values can be visualised below in Figure 23. The low MFI values can be due to various factors such as growing conditions of the tumour cell lines might have somewhat affected the liposomal uptake. Another factor that could affect the uptake is the complexity of the individual variables within the optimal liposome preparation. However, the actual MFI values are of value with high liposomal uptake observed.

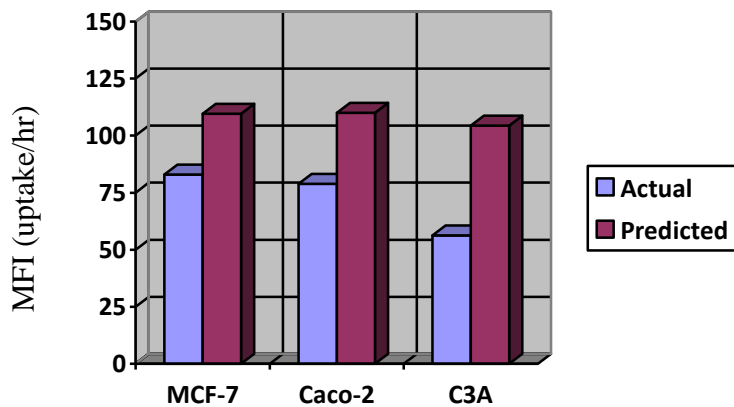


Figure 23: Comparison of predicted and actual values of liposomal uptake into MCF-7, Caco-2 and C3A cell lines

4.3.2 Characterisation of liposomes

4.3.2.1 Photon correlation spectroscopy

The particle size and zeta potential analysis of the optimised batch was performed on a Zetasizer™ using photon correlation spectroscopy. The results are shown in Table 9 below. As described in the statistical design for the optimised batch, liposomes had to be filtered and sized utilising a 200 nm polycarbonate membrane filters. After passing the optimised liposome solution through the filter, particle size and zeta potential analysis were performed. The results obtained have shown to be adequate. The average particle size of the optimised batch was 113.9 nm with a standard deviation of ± 0.86 . This has shown that the liposomes have a slight variation in their size and the method employed in producing the liposome has proved to be successful. The zeta potential of the optimised liposome batch was shown to be -28.20, which is equally negative. The negative zeta potential value obtained from the results can be due to the negatively charged nature of the PS

phospholipid. In addition, CHEMS also has the ability to influence the zeta potential result due to CHEMS adopting an anionic state.

Table 9: Representation of average particle size, polydispersity index and zeta potential of the optimised liposome batch			
Batch	Average particle size (nm)	Average polydispersity index (PI)*	Average zeta potential (mV)
Optimised batch	113.9 (± 0.86)	0.137 (± 0.006)	-28.20 (± 0.115)
*PI represents the polydispersity index used as indication of size distribution of vesicles			

4.3.2.2 Atomic force microscopy (AFM)

Physical characterisation of the optimal liposome preparation was performed using AFM equipped with ScanAsyst. The liposome preparation was imaged with a mica sheet used as a solid substrate in order to allow the liposome to be stable under imaging conditions. The image of the liposome captured on the mica sheet is shown in Figure 24. AFM images taken in tapping mode in air allows images of the liposomal morphology to be captured without staining or sample manipulations. The advantage of using the AFM in tapping mode allows images to be taken at high resolution as well as eliminates the lateral and shear forces that can break or deform the liposome shape. AFM images were obtained on the optimal liposome preparation. Images were taken immediately after preparation. In Figure 24, the mean sizes of the liposomes from A to E were calculated to be 144.50 nm. The measured liposome size ranged from 130.82 nm to 162.36 nm. The obtained results are shown in Figure 24, and clearly indicate that liposomes sizes ranged between

the expected size ranges of < 200 nm and correlate reasonably with the results obtained using photon correlation spectroscopy.

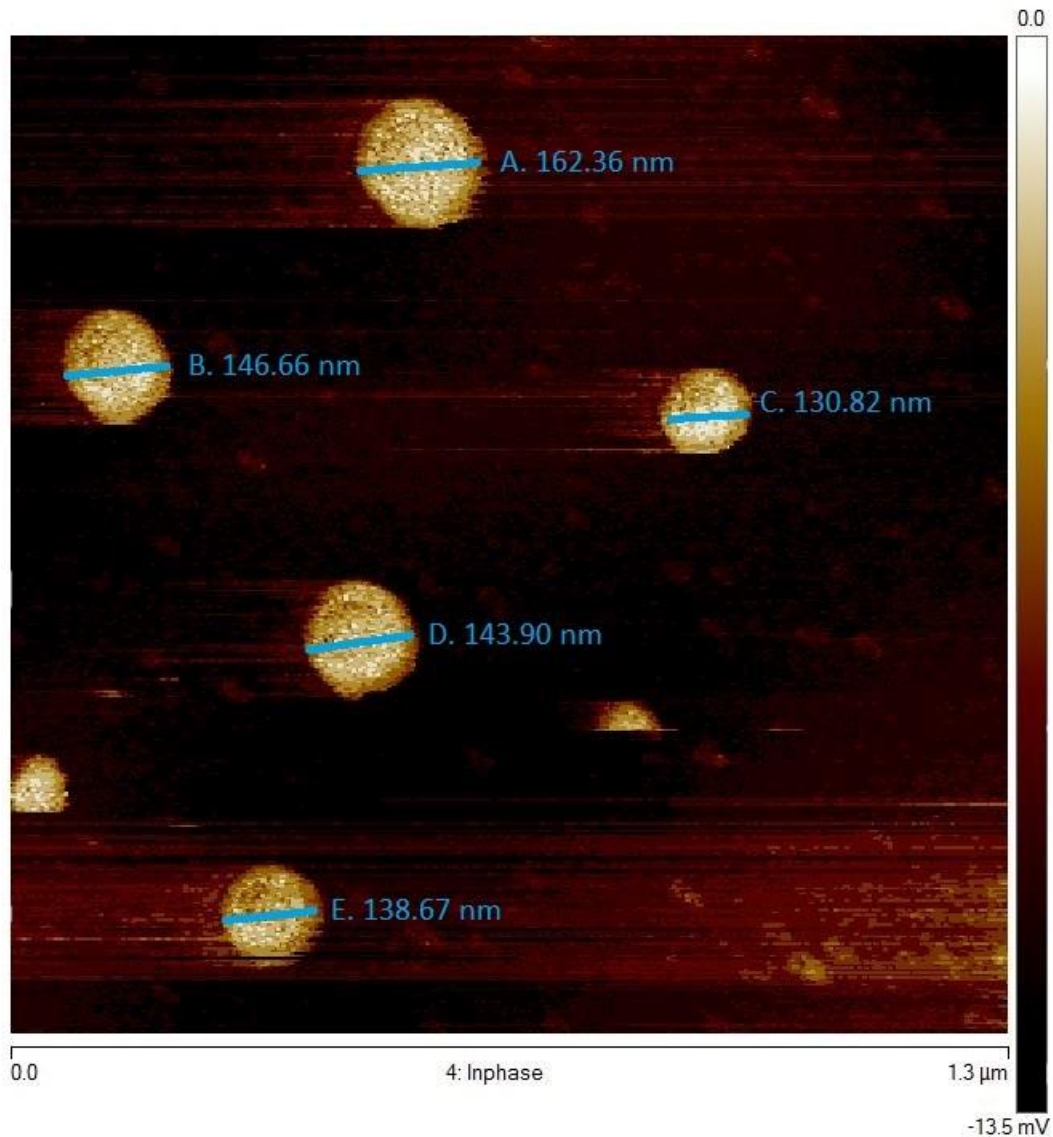


Figure 24: AFM image of the optimised liposome batch captured in noncontact mode. Liposomes A-E are images of the actual liposomes captured with the AFM in air (images acquired within 30 minutes of sample deposition on mica sheet).

4.3.3 Intracellular delivery of liposome

4.3.3.1 Flow cytometry analysis

Flow cytometry analysis was carried out on the optimal liposome preparation. The experimental runs were performed in triplicate on the MCF-7, Caco-2 and C3A cell lines. Liposomes were attached with 1,2-dioleoyl-sn-glycero-3-phosphoethanolamine-N-(carboxyfluorescein)(PE-CF) head group in order to make the liposomes fluoresce at green light. An outlier test was performed on the MFI results obtained from the flow cytometer using Grubb's outlier test (GraphPad® software) (GraphPad, 2015). This outlier test was used to eliminate any results that did not fit the trending results obtained. For the MCF-7 and Caco-2 cell lines, it was established that there were no outliers present in the MFI results. However, the C3A cell line contained an outlier with a MFI value of 145 (Table 11). Therefore the result was excluded from the average calculation to give a true reflection of the MFI and uptake of the optimal liposome preparation in the C3A cell line.

A graphical representation of the uptake of liposomes is shown in Figure 25. Graphs A, B & C are the quantified data for uptake of liposomes for MCF-7, Caco-2 and C3A cell lines respectively. The average of the mean fluorescence intensity (MFI) for the cell lines was calculated and is presented in Table 10. The average MFI for the MCF-7 and Caco-2 cell line was calculated to be 82.94 and 78.90 respectively. However, the average MFI for the C3A cell lines was calculated to be 56.33, which is a much lower value compared to the other two cell lines, thus indicating that the liposome preparation was not taken up as efficiently. This result correlates with Figure 24C, where the fluorescent peak (on the right) can be seen to have a lesser shift to the right than the above MCF-7 and Caco-2 cell lines. The C3A cell line can

also be seen to have a significantly lower number of gated events, thus indicating that the liposomes have not been taken up efficiently. The MCF-7 and Caco-2 cell lines have higher MFI values which can be correlated with Figures 25A and B. The colour peaks on the graph of the treated cell lines have shifted further to the right indicating an intense fluorescence observation. Therefore, MCF-7 and Caco-2 cell lines show a greater correlation to the predicted model for the optimal liposome preparation compared to the C3A cell line.

Table 10: Representation of the mean fluorescence intensity (MFI) results for the optimised liposome batch in flow cytometry for MCF-7 cell line.										
Optimised batch										
X mean										Average
Control	1.24	1	1.11	1.58	1.23	1.04	2.18	1.95	1.17	1.40
MFI	108	97.5	69.2	128	116	115	41.6	32.2	39	82.94

Table 11: Representation of the mean fluorescence intensity (MFI) results for the optimised liposome batch in flow cytometry for Caco-2 cell line										
Optimised batch										
X mean										Average
Control	1.01	1.6	1.47	1.03	0.83	0.835	0.922	0.892	0.896	1.05
MFI	110	113	102	94.2	92.8	72.2	42.8	42.4	40.6	78.90

Table 12: Representation of the mean fluorescence intensity (MFI) results for the optimised liposome batch in flow cytometry for C3A cell line.										
Optimised batch										
X mean										Average
Control	1.42	1.8	1.11	2.62	1.85	2.12	3.77	2.42	2.49	2.17
MFI	50	37.9	37.2	66.6	41.3	48.1	96.3	(145)*	73.3	56.33
*excluded from average calculation (outlier)										

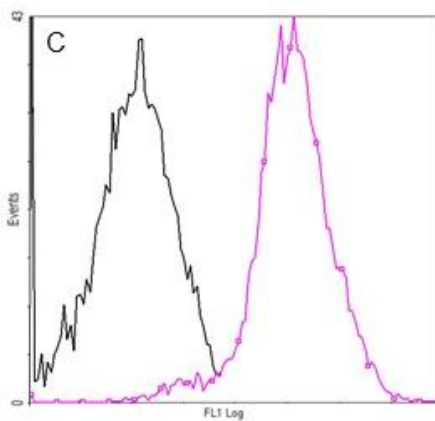
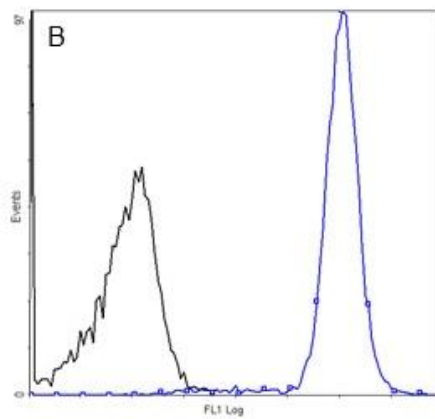
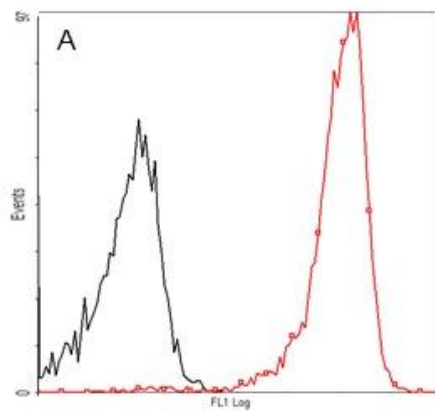


Figure 25: Graphical representation of the flow cytometry analysis of the optimal liposome preparation. A: MCF-7, B: Caco-2 and C: C3A. Tests were performed in triplicate. Black peak is the control.

4.3.3.2 Fluorescence microscopy analysis

The fluorescence microscopy images below represent the uptake of the optimal liposomes into MCF-7, Caco-2 and C3A cell lines respectively. Fluorescence microscopy was used to observe the cellular uptake of the optimal liposome preparation into the tumour cell lines. After reaching 70 – 80 % confluency of the cell lines, the desired cell wells were used for liposome visualisation by transferring 100 μ L of optimal liposome preparation into the cell wells. For the fluorescence microscopy, duplicate wells were prepared for each cell lines, one that was treated with the optimal liposome preparation and the other well was used a control (untreated). The tumour cell lines were exposed to the optimised liposomes for one hour at 37 °C and washed three times prior to visualisation in order to remove the excess liposome solution, after which fluorescent images were captured and shown in Figures 26, 27 and 28. It can be understood from the fluorescent images that the optimised liposomes have been successfully taken up into the tumour cells. The liposomes can be seen to be concentrated around the membranes of the tumour cell lines thus indicating a significant amount of membrane fusion between the liposomes and the tumour cell lines had occurred.

However, although fluorescence can be observed on the membranes of all three tumour cell lines, the MCF-7 and Caco-2 cell lines can be seen to have a brighter fluorescence presence compared to the C3A cell line. The C3A cell line can be seen to have taken up much less of the liposomes and this could be due to the nature of the cell line as well as the growth pattern of the cells. C3A cells tend to form clusters when grown, thus making it much more difficult for liposomes to fuse or be internalised by the tumour cell line. The results obtained from the flow cytometry

analysis directly correlates with the fluorescent images taken of the three cell lines, in which MCF-7 and Caco-2 cell lines have a higher MFI compared to the C3A cell line. Fluorescence of the tumour cell line membrane can be seen in Figures 26, 27 and 28 and this can be due to the liposomes having the ability to destabilise in the acidic environment of the tumours and thus fusing with the tumour cell membranes.

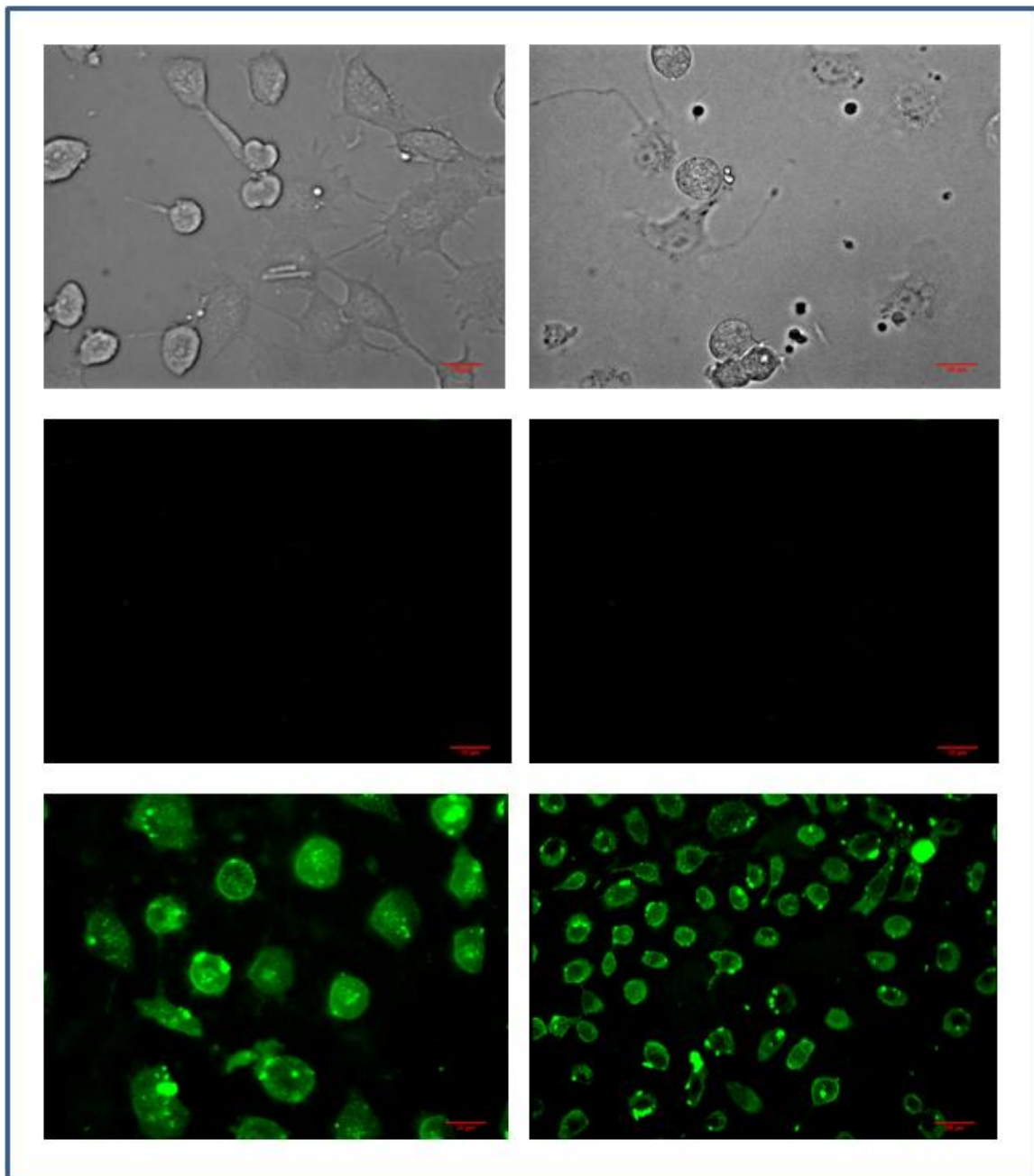


Figure 26: Fluorescence microscopy of MCF-7 cell line treated with the optimal liposome preparation. Cells were grown to 70-80 % confluence and treated for 1 hour. Top images – bright field (untreated); middle images – control; bottom images – fluorescence (treated).

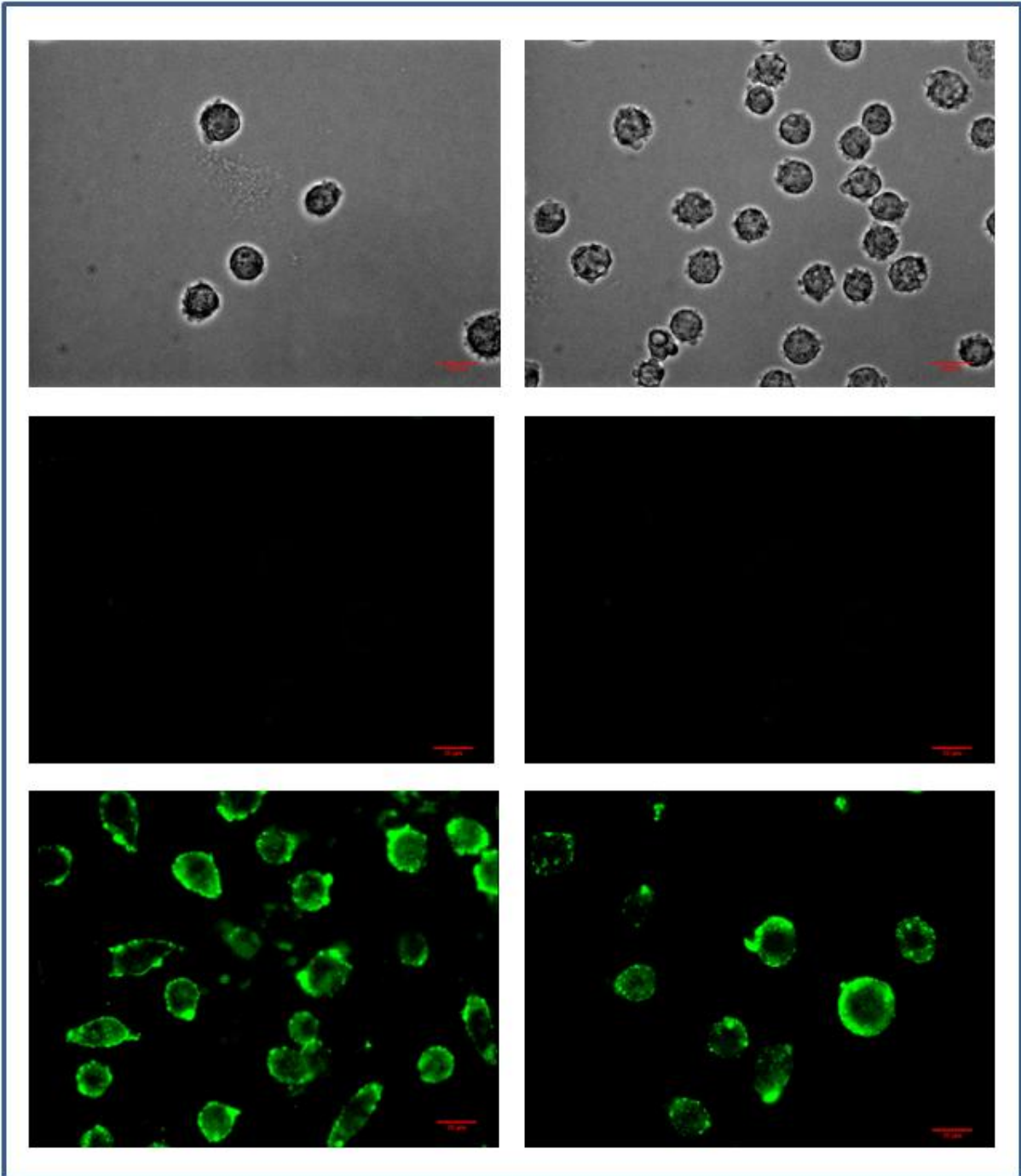


Figure 27: Fluorescence microscopy of Caco-2 cell line treated with the optimal liposome preparation. Cells were grown to 70-80 % confluence and treated for 1 hour. Top images – bright field (untreated); middle images – control; bottom images – fluorescence (treated).

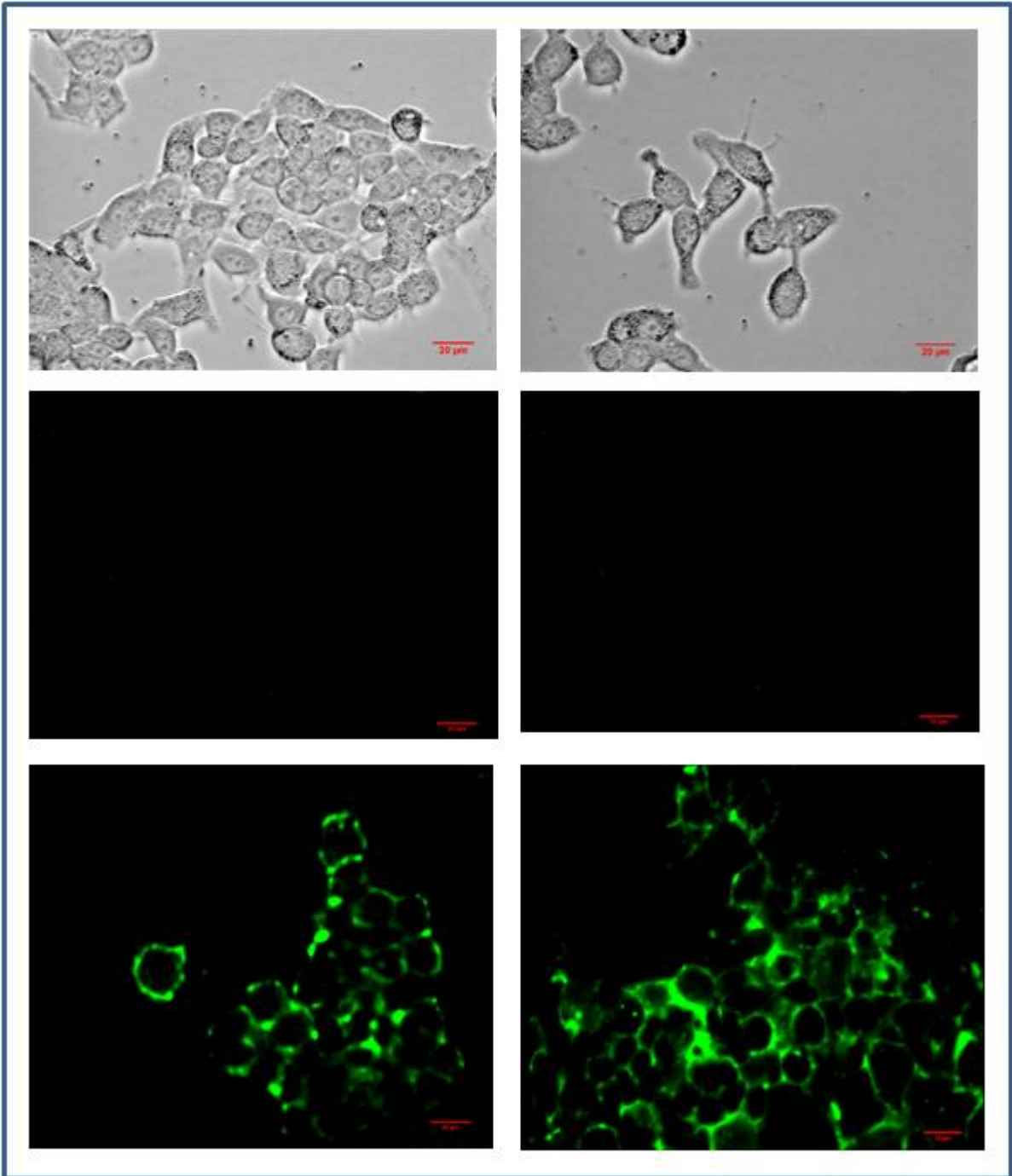


Figure 28: Fluorescence microscopy of C3A cell line treated with the optimal liposome preparation. Cells were grown to 70-80 % confluence and treated for 1 hour. Top images – bright field (untreated); middle images – control; bottom images – fluorescence (treated).

The results obtained thus indicates that the optimised liposomes prepared have the ability to fuse with the membranes of the tumour cells. The data presented from the statistical design can be seen to be efficient and useful in the optimisation of a liposome preparation that has the capability to fuse with the membranes of the tumour cell lines. The uptake of the liposomes indicates that the optimised liposome preparation can be vital in fusing with the tumour cell membranes without having to utilise targeting molecules or cell penetrating peptides. Early research has shown that antibody-targeted liposomes have increased selectivity and interaction with the targeted tissue (Allen and Cullis, 2013). However, the modified liposomes were being rapidly eliminated from the blood circulation resulting in limited effects of the encapsulated molecules. This problem was then resolved by the introduction of PEG onto the surface of the liposomes which then increased the blood circulation. Although the introduction of PEG somewhat increased the antibody-targeted liposomes, the methods for producing these liposomes are tedious and very difficult to regulate (Allen and Cullis, 2013). The surface modification of liposomes can thus be poorly controlled, resulting in their rapid elimination by the RES.

Research has shown that passive delivery of liposomes with the ability to release drug molecules near or at the tumour site results in anti-cancer activity. Hence, the ability for liposomes to fuse with the tumour cell membranes and deliver a payload of drug molecules directly into the tumour cell would result in an astounding increase in anti-cancer activity (Allen and Cullis, 2013). Studies have shown that targeted and non-targeted liposomes follow the same distribution pathway when being delivered to the site of action and targeting liposomes share the same half-life as those that are not targeted (Allen and Cullis, 2013). Most of the emphasis is not placed on the

ability of liposomes to be targeted but rather the ability of the liposome to have an efficient drug release rate at the site of action. Therefore fusogenic liposomes have the ability to release their entrapped drug molecules directly into the tumour site after fusion with the tumour cell membranes which makes these liposomes extremely advantageous in increasing anti-tumour effects.

Chapter 5: Conclusions and Recommendations

The variables used in the study were identified from literature as being the most suitable factors in preparing liposome that have the ability to fuse with MCF-7, Caco-2 and C3A cell line membranes. The four factors chosen from literature were the phospholipid type (PS or DOPE), the concentration of cholesteryl hemisuccinate (CHEMS) (10 – 40 %), the concentration of PEG₂₀₀₀-PE (0.5 – 4 %) and liposome size (100 or 200 nm).

The variables were subjected to primary screening using a 2^{4-1} fractional factorial design. Eight experimental runs at different liposome preparations were performed in order to determine which variables would be best suited in order to navigate the design space. Flow cytometry analysis was performed and the results were plotted as a value of MFI uptake per hour, which was shown to have high levels of uptake on all three cell lines. The ANOVA analysis performed on the statistical design method for all three cell lines have to have a significant p-value of <0.05. Thus, indicating that the variables used in the experimental design were capable of navigating the design space. Liposomes prepared using phospholipid type PS has showed high levels of MFI on all three cell lines compared to phospholipid DOPE.

Therefore, the optimal liposome preparation chosen following statistical analysis consisted of phospholipid type PS, 22.91 % of CHEMS, 4 % of PEG₂₀₀₀-PE and a liposome size of 200 nm. Atomic force microscopy analysis has shown that the method of liposome preparation and formulation were successful in creating the desired liposomes of 200 nm. Fluorescence microscopy has shown that the optimal liposome formulation was optimal in achieving liposomes that have the ability to fuse

tumour cell line membranes as it can be seen from the images that high levels of liposomes are observed on the membranes of the tumour cell lines. This was further emphasised with the high levels of MFI, although the actual MFI readings below the predicted MFI values set out by the statistical design. This could be due to variability of the liposome batch and complexity of the liposome preparation.

The notable finding of the optimal batch proposed by the statistical design model was the use of 200 nm sized liposomes. It can be seen that 200 nm sized liposomes have the ability to be taken up more effectively than 100 nm sized liposomes which was one of the significant conclusions of the study. Another finding was the fact that liposomes prepared using PS had more desirability for uptake into all tumour cell lines tested, which originated from cancer tissue compared to DOPE. Therefore, the variables chosen from literature and the statistical design model used in the study has shown to be significant in attaining an optimal liposome preparation for fusion with tumour cell line membranes.

For future studies, it would be ideal to prepare these liposomes and encapsulate anti-cancer drug molecules. Studies such as: drug encapsulation and membrane leakages could be performed in order to test the stability and rigidity of the liposomes. I would recommend that the liposomes containing the encapsulated drug molecules be tested for anti-cancer activity on MCF-7, Caco-2 and C3A cell lines. Thereafter it would also be significantly beneficial if these drug encapsulated molecules would be tested *in vivo* in order to ascertain their advantages and effects in anti-cancer therapy.

References

- Akbarzadeh, A., Rezaei-Sadabady, R., Davaran, S., Joo, S. W., Zarghami, N., Hanifehpour, Y., Samiei, M., Kouhi, M. & Nejati-Koshki, K. 2013. Liposome: classification, preparation, and applications. *Nanoscale Research Letters*, 8, 102.
- Alexis, F., Rhee, J., Richie, J., Radovic-Moreno, A., Langer, R. And Farokhzad, O. 2008. New frontiers in nanotechnology for cancer treatment. *Urologic Oncology: Seminars and Original Investigations*, 26(1), 74-85.
- Allen, T. M., & Cullis, P. R. 2013. Liposomal drug delivery systems: from concept to clinical applications. *Advanced Drug Delivery Reviews*, 65(1), 36-48.
- Allison, A. & Gregoriadis, G. 1974. Liposomes as immunological adjuvants. *Nature*, 252(5480), 252-252.
- Bangham, A., Standish, M. M. & Watkins, J. 1965. Diffusion of univalent ions across the lamellae of swollen phospholipids. *Journal of Molecular Biology*, 13, 238-252.
- Bhadra, D., Bhadra, S., Jain, S. & Jain, N. 2003. A PEGylated dendritic nanoparticulate carrier of fluorouracil. *International Journal of Pharmaceutics*, 257, 111-124.
- Blomme, S. 2008. *Toxicological evaluation of liposomal antimicrobials*. Ottawa: Library and Archives Canada = Bibliothèque et Archives Canada.
- Cailleau, R., Olivé, M. and Cruciger, Q. 1978. Long-term human breast carcinoma cell lines of metastatic origin: Preliminary characterization. *In Vitro*, 14(11), 911-915.

- Cargillfoods. 2015. *Cargill Food and Beverage Ingredients EMEA: Products - Lecithins - Functionality*. [online] Available at: <http://www.cargillfoods.com/emea/en/products/lecithins/functionality/index.jsp>. [Accessed 27 Nov. 2015].
- Carrel, A. & Burrows, M. 1911. Cultivation in vitro of malignant tumors. *Journal of Experimental Medicine*, 13(5), 571-575.
- Carozzi, V., Canta, A. & Chiorazzi, A. 2015. Chemotherapy-induced peripheral neuropathy: What do we know about mechanisms? *Neuroscience Letters*, 596, 90-107.
- Cattel, L., Ceruti, M. & Dosio, F. 2002. From conventional to stealth liposomes: a new frontier in cancer chemotherapy. *Tumori*, 89, 237-249.
- Cancer Research UK. 2015. *Cancers in general*. [online] Available at: <http://www.cancerresearchuk.org> [Accessed 26 Oct. 2015].
- Chan, W. C., Maxwell, D. J., Gao, X., Bailey, R. E., Han, M. & Nie, S. 2002. Luminescent quantum dots for multiplexed biological detection and imaging. *Current Opinion in Biotechnology*, 13, 40-46.
- Chan, W. C. & Nie, S. 1998. Quantum dot bioconjugates for ultrasensitive nonisotopic detection. *Science*, 281, 2016-2018.
- Christenson, E. S., James, T., Agrawal, V. & Park, B. H. 2015. Use of biomarkers for the assessment of chemotherapy-induced cardiac toxicity. *Clinical Biochemistry*, 48, 223-235.
- Cullis, P. & De Kruijff, B. 1978. The polymorphic phase behaviour of phosphatidylethanolamines of natural and synthetic origin. A ³¹P NMR study. *Biochimica et Biophysica Acta (BBA)-Biomembranes*, 513, 31-42.

- Dawar, S., Singh, N., Kanwar, R. K., Kennedy, R. L., Veedu, R. N., Zhou, S.-F., Krishnakumar, S., Hazra, S., Sasidharan, S. & Duan, W. 2013. Multifunctional and multitargeted nanoparticles for drug delivery to overcome barriers of drug resistance in human cancers. *Drug Discovery Today*, 18, 1292-1300.
- De La Fuente, M., Langer, R. & Alonso, M. J. 2014. Nanotechnology Approaches for Cancer Immunotherapy and Immunomodulation. *Nano-Oncologicals*, 215-242.
- De Martel, C., Ferlay, J., Franceschi, S., Vignat, J., Bray, F., Forman, D. & Plummer, M. 2012. Global burden of cancers attributable to infections in 2008: a review and synthetic analysis. *The Lancet Oncology*, 13, 607-615.
- Deol, P. & Khuller, G. 1997. Lung specific stealth liposomes: stability, biodistribution and toxicity of liposomal antitubercular drugs in mice. *Biochimica et Biophysica Acta (BBA)-General Subjects*, 1334, 161-172.
- Dietrich, J., Prust, M. & Kaiser, J. 2015. Chemotherapy, cognitive impairment and hippocampal toxicity. *Neuroscience*, 309, 224-232.
- Drexler, K. E., Peterson, C. & Pergamit, G. 1991. *Unbounding the future. William Morrow, New York*, 294.
- Drummond, D. C., Meyer, O., Hong, K., Kirpotin, D. B., & Papahadjopoulos, D. 1999. Optimizing liposomes for delivery of chemotherapeutic agents to solid tumors. *Pharmacological Reviews*, 51(4), 691-744.
- Dua, J., Rana, A. & Bhandari, A. 2012. Liposome: methods of preparation and applications. *International Journal of Pharmaceutical Studies and Research*, 3, 14-20.
- Düzgüneş, N. & Nir, S. 1999. Mechanisms and kinetics of liposome–cell interactions. *Advanced Drug Delivery Reviews*, 40, 3-18.

- Edwards, S.A. 2006. *The nanotech pioneers*. Weinheim: Wiley-VCH.
- Ekimov, A., Efros, A. L. & Onushchenko, A. 1985. Quantum size effect in semiconductor microcrystals. *Solid State Communications*, 56, 921-924.
- Elbayoumi, T. & Torchilin, V. 2010. Current Trends in Liposome Research. *Methods in Molecular Biology*, 605, 1-27.
- Emanuel, N., Kedar, E., Bolotin, E. M., Smorodinsky, N. I. & Barenholz, Y. 1996. Preparation and characterization of doxorubicin-loaded sterically stabilized immunoliposomes. *Pharmaceutical Research*, 13, 352-359.
- Emerich, D. F. & Thanos, C. G. 2003. Nanotechnology and medicine. *Expert Opinion on Biological Therapy*, 3, 655-663.
- Evjen, T. J., Nilssen, E. A., Røgnvaldsson, S., Brandl, M. & Fossheim, S. L. 2010. Distearoylphosphatidylethanolamine-based liposomes for ultrasound-mediated drug delivery. *European Journal of Pharmaceutics and Biopharmaceutics*, 75, 327-333.
- Ferlay, J., Shin, H. R., Bray, F., Forman, D., Mathers, C. & Parkin, D. M. 2010. Estimates of worldwide burden of cancer in 2008: GLOBOCAN 2008. *International Journal of Cancer*, 127, 2893-2917.
- Feynman, R. P. 1960. There's plenty of room at the bottom. *Engineering and Science*, 23, 22-36.
- Fonseca, N. A., Gregório, A. C., Valério-Fernandes, Â., Simões, S. & Moreira, J. N. 2014. Bridging cancer biology and the patients' needs with nanotechnology-based approaches. *Cancer Treatment Reviews*, 40, 626-635.
- Gabizon, A., Dagan, A., Goren, D., Barenholz, Y. & Fuks, Z. 1982. Liposomes as in vivo carriers of adriamycin: reduced cardiac uptake and preserved antitumor activity in mice. *Cancer Research*, 42, 4734-4739.

- Genç, R. K., Ortiz, M. & O' Sullivan, C. K. 2009. Curvature-tuned preparation of nanoliposomes. *Langmuir*, 25, 12604-12613.
- Gerasimov, O. V., Boomer, J. A., Qualls, M. M. & Thompson, D. H. 1999. Cytosolic drug delivery using pH-and light-sensitive liposomes. *Advanced Drug Delivery Reviews*, 38, 317-338.
- GraphPad. 2015. *GraphPad QuickCalcs: outlier calculator*. [online] Available at: <http://graphpad.com/quickcalcs/grubbs1/>. [Accessed 19 Aug. 2015].
- Gupta, A. S. 2011. Nanomedicine approaches in vascular disease: a review. *Nanomedicine: Nanotechnology, Biology and Medicine*, 7, 763-779.
- Gupta, U., Agashe, H. B., Asthana, A. & Jain, N. K. 2006. A review of in vitro–in vivo investigations on dendrimers: the novel nanoscopic drug carriers. *Nanomedicine: Nanotechnology, Biology and Medicine*, 2, 66-73.
- Hafez, I. M. & Cullis, P. R. 2001. Roles of lipid polymorphism in intracellular delivery. *Advanced Drug Delivery Reviews*, 47, 139-148.
- Han, M., Gao, X., Su, J. Z. & Nie, S. 2001. Quantum-dot-tagged microbeads for multiplexed optical coding of biomolecules. *Nature Biotechnology*, 19, 631-635.
- Hauert, S. & Bhatia, S. N. 2014. Mechanisms of cooperation in cancer nanomedicine: towards systems nanotechnology. *Trends in Biotechnology*, 32, 448-455.
- Hauser, H. & Gains, N. 1982. Spontaneous vesiculation of phospholipids: a simple and quick method of forming unilamellar vesicles. *Proceedings of the National Academy of Sciences*, 79, 1683-1687.
- Holliday, D. and Speirs, V. 2011. Choosing the right cell line for breast cancer research. *Breast Cancer Research*, 13(4), 215.

- Iijima, S. 1991. Helical microtubules of graphitic carbon. *Nature*, 354, 56-58.
- Kanter, P., Bullard, G., Pilkiewicz, F., Mayer, L., Cullis, P. & Pavelic, Z. 1992. Preclinical toxicology study of liposome encapsulated doxorubicin (TLC D-99): comparison with doxorubicin and empty liposomes in mice and dogs. *In vivo (Athens, Greece)*, 7, 85-95.
- Kim, M. G., Park, J. Y., Shon, Y., Kim, G., Shim, G., & Oh, Y. K. 2014. Nanotechnology and vaccine development. *asian journal of pharmaceutical sciences*, 9(5), 227-235.
- Kono, K., Iwamoto, M., Nishikawa, R., Yanagie, H. & Takagishi, T. 2000. Design of fusogenic liposomes using a poly (ethylene glycol) derivative having amino groups. *Journal of Controlled Release*, 68, 225-235.
- Koo, O. M., Rubinstein, I. & Onyuksel, H. 2005. Role of nanotechnology in targeted drug delivery and imaging: a concise review. *Nanomedicine: Nanotechnology, Biology and Medicine*, 1, 193-212.
- Koshkaryev, A., Piroyan, A. & Torchilin, V. P. 2013. Bleomycin in octaarginine-modified fusogenic liposomes results in improved tumor growth inhibition. *Cancer Letters*, 334, 293-301.
- Kreuter, J. & Speiser, P. P. 1976. In vitro studies of poly (methyl methacrylate) adjuvants. *Journal of Pharmaceutical Sciences*, 65, 1624-1627.
- Kroto, H. W., Heath, J. R., O'brien, S. C., Curl, R. F. & Smalley, R. E. 1985. C 60: buckminsterfullerene. *Nature*, 318, 162-163.
- Kuo, Y.C. & Chen, H.H. 2006. Effect of nanoparticulate polybutylcyanoacrylate and methylmethacrylate–sulfopropylmethacrylate on the permeability of zidovudine and lamivudine across the in vitro blood–brain barrier. *International Journal of Pharmaceutics*, 327, 160-169.

- Lai, M. Z., Duzgunes, N. & Szoka, F. C. 1985a. Effects of replacement of the hydroxyl group of cholesterol and tocopherol on the thermotropic behavior of phospholipid membranes. *Biochemistry*, 24, 1646-1653.
- Lai, M. Z., Vail, W. J. & Szoka, F. C. 1985b. Acid-and calcium-induced structural changes in phosphatidylethanolamine membranes stabilized by cholesteryl hemisuccinate. *Biochemistry*, 24, 1654-1661.
- Lasic, D. D. & Papahadjopoulos, D. 1996. Liposomes and biopolymers in drug and gene delivery. *Current Opinion in Solid State and Materials Science*, 1, 392-400.
- Levenson, A. S., & Jordan, V. C. 1997. MCF-7: the first hormone-responsive breast cancer cell line. *Cancer Research*, (57), 3071-8.
- Leander, P., Höglund, P., Borseth, A., Kloster, Y. & Berg, A. 2001. A new liposomal liver-specific contrast agent for CT: first human phase-I clinical trial assessing efficacy and safety. *European Radiology*, 11, 698-704.
- Lee, B. K., Yun, Y. H. & Park, K. 2014. Smart nanoparticles for drug delivery: Boundaries and opportunities. *Chemical Engineering Science*.
- Lee, P.C., Chiou, Y.C., Wong, J.M., Peng, C.L. & Shieh, M.J. 2013. Targeting colorectal cancer cells with single-walled carbon nanotubes conjugated to anticancer agent SN-38 and EGFR antibody. *Biomaterials*, 34, 8756-8765.
- Leonard, R., Williams, S., Tulpule, A., Levine, A. & Oliveros, S. 2009. Improving the therapeutic index of anthracycline chemotherapy: Focus on liposomal doxorubicin (Myocet™). *The Breast*, 18, 218-224.
- Liu, M., Kono, K. & Fréchet, J. M. 2000. Water-soluble dendritic unimolecular micelles: Their potential as drug delivery agents. *Journal of Controlled Release*, 65, 121-131.

- Macdonald, R. C., Macdonald, R. I., Menco, B. P. M., Takeshita, K., Subbarao, N. K. & Hu, L.-R. 1991. Small-volume extrusion apparatus for preparation of large, unilamellar vesicles. *Biochimica et Biophysica Acta (BBA)-Biomembranes*, 1061, 297-303.
- Magee, W. E., Goff, C. W., Schoknecht, J., Smith, M. D. & Cherian, K. 1974. The interaction of cationic liposomes containing entrapped horseradish peroxidase with cells in culture. *The Journal of Cell Biology*, 63, 492-504.
- Maguire, C. M., Mahfoud, O. K., Rakovich, T., Gerard, V. A., Prina-Mello, A., Gun'ko, Y. & Volkov, Y. 2014. Heparin conjugated quantum dots for in vitro imaging applications. *Nanomedicine: Nanotechnology, Biology and Medicine*, 10, 1853-1861.
- Makin, G. 2014. Principles of chemotherapy. *Paediatrics and Child Health*, 24, 161-165.
- Malik, N., Evagorou, E. G. & Duncan, R. 1999. Dendrimer-platinate: a novel approach to cancer chemotherapy. *Anti-Cancer Drugs*, 10, 767-776.
- Nanjwade, B. K., Bechra, H. M., Derkar, G. K., Manvi, F. & Nanjwade, V. K. 2009. Dendrimers: emerging polymers for drug-delivery systems. *European Journal of Pharmaceutical Sciences*, 38, 185-196.
- Nanjwade, B. K., Singh, J., Parikh, K. A. & Manvi, F. 2010. Preparation and evaluation of carboplatin biodegradable polymeric nanoparticles. *International Journal of Pharmaceutics*, 385, 176-180.
- National Cancer Institute. 2015. *Cancer Treatment*. [online] Available at: <http://www.cancer.gov/about-cancer/treatment> [Accessed 12 Aug. 2015].

- Orive, G., Hernandez, R. M., Gascón, A. R. G., Domínguez-Gil, A. & Pedraz, J. L. 2003. Drug delivery in biotechnology: present and future. *Current Opinion in Biotechnology*, 14, 659-664.
- Park, J., Kirpotin, D., Hong, K., Shalaby, R., Shao, Y., Nielsen, U., Marks, J., Papahadjopoulos, D. & Benz, C. 2001. Tumor targeting using anti-her2 immunoliposomes. *Journal of Controlled Release*, 74, 95-113.
- Parveen, S., Misra, R. & Sahoo, S. K. 2012. Nanoparticles: a boon to drug delivery, therapeutics, diagnostics and imaging. *Nanomedicine: Nanotechnology, Biology and Medicine*, 8, 147-166.
- Peretz, S. & Regev, O. 2012. Carbon nanotubes as nanocarriers in medicine. *Current Opinion in Colloid & Interface Science*, 17, 360-368.
- Perry, J. L., Martin, C. R. & Stewart, J. D. 2011. Drug-Delivery Strategies by Using Template-Synthesized Nanotubes. *Chemistry-A European Journal*, 17, 6296-6302.
- Renshaw, P. F., Janoff, A. S. & Miller, K. W. 1983. On the nature of dilute aqueous cholesterol suspensions. *Journal of Lipid Research*, 24, 47-51.
- Quaroni, A. and Hochman, J. 1996. Development of intestinal cell culture models for drug transport and metabolism studies. *Advanced Drug Delivery Reviews*, 22(1-2), 3-52.
- Sachse, A., Leike, J. U., Röling, G. L., Wagner, S. E. & Krause, W. 1993. Preparation and evaluation of lyophilized iopromide-carrying liposomes for liver tumor detection. *Investigative Radiology*, 28, 838-844.
- Safari, J. & Zarnegar, Z. 2014. Advanced drug delivery systems: Nanotechnology of health design A review. *Journal of Saudi Chemical Society*, 18, 85-99.

- Sahoo, S., Parveen, S. & Panda, J. 2007. The present and future of nanotechnology in human health care. *Nanomedicine: Nanotechnology, Biology and Medicine*, 3, 20-31.
- Sambuy, Y., De Angelis, I., Ranaldi, G., Scarino, M., Stamatii, A. and Zucco, F. 2005. The Caco-2 cell line as a model of the intestinal barrier: influence of cell and culture-related factors on Caco-2 cell functional characteristics. *Cell Biology Toxicology*, 21(1), 1-26.
- Sawant, R. R. & Torchilin, V. P. 2012. Challenges in development of targeted liposomal therapeutics. *The AAPS journal*, 14, 303-315.
- Scherer, W. F., Syverton, J. T., & Gey, G. O. 1953. Studies on the propagation in vitro of poliomyelitis viruses IV. Viral multiplication in a stable strain of human malignant epithelial cells (strain HeLa) derived from an epidermoid carcinoma of the cervix. *The Journal of Experimental Medicine*, 97(5), 695-710.
- Schipper, M. L., Nakayama-Ratchford, N., Davis, C. R., Kam, N. W. S., Chu, P., Liu, Z., Sun, X., Dai, H. & Gambhir, S. S. 2008. A pilot toxicology study of single-walled carbon nanotubes in a small sample of mice. *Nature Nanotechnology*, 3, 216-221.
- Sharma, A. & Sharma, U. S. 1997. Liposomes in drug delivery: progress and limitations. *International Journal of Pharmaceutics*, 154, 123-140.
- Shim, G., Kim, M.G., Park, J. Y. & Oh, Y.K. 2013. Application of cationic liposomes for delivery of nucleic acids. *Asian Journal of Pharmaceutical Sciences*, 8, 72-80.
- Simoës, S., Slepishkin, V., Düzgünes, N. & Pedroso De Lima, M. C. 2001. On the mechanisms of internalization and intracellular delivery mediated by pH-

- sensitive liposomes. *Biochimica et Biophysica Acta (BBA)-Biomembranes*, 1515, 23-37.
- Sjoblom, B., Gronberg, B. H., Benth, J. S., Baracos, V. E., Flotten, O., Hjermsstad, M. J., Aass, N. & Jordhoy, M. 2015. Low muscle mass is associated with chemotherapy-induced haematological toxicity in advanced non-small cell lung cancer. *Lung Cancer*, 90, 85-91.
- Svenson, S. 2009. Dendrimers as versatile platform in drug delivery applications. *European Journal of Pharmaceutics and Biopharmaceutics*, 71, 445-462.
- Tilcock, C. 1999. Delivery of contrast agents for magnetic resonance imaging, computed tomography, nuclear medicine and ultrasound. *Advanced Drug Delivery Reviews*, 37, 33-51.
- Tomalia, D. A., Baker, H., Dewald, J., Hall, M., Kallos, G., Martin, S., Roeck, J., Ryder, J. & Smith, P. 1985. A new class of polymers: starburst-dendritic macromolecules. *Polymer Journal*, 17, 117-132.
- Torchilin, V. P. 2005. Recent advances with liposomes as pharmaceutical carriers. *Nature Reviews Drug Discovery*, 4, 145-160.
- Torchilin, V. P. 2012. Multifunctional nanocarriers. *Advanced drug delivery reviews*, 64, 302-315.
- Tran, P. A., Zhang, L. & Webster, T. J. 2009. Carbon nanofibers and carbon nanotubes in regenerative medicine. *Advanced Drug Delivery Reviews*, 61, 1097-1114.
- van Marion, D., Domanska, U., Timmer-Bosscha, H. & Walenkamp, A. 2015. Studying cancer metastasis: Existing models, challenges and future perspectives. *Critical Reviews in Oncology/Hematology*.

- Vasir, J. K., Reddy, M. K. & Labhasetwar, V. D. 2005. Nanosystems in drug targeting: opportunities and challenges. *Current Nanoscience*, 1, 47-64.
- Walde, P. & Ichikawa, S. 2001. Enzymes inside lipid vesicles: preparation, reactivity and applications. *Biomolecular Engineering*, 18, 143-177.
- Whitcomb, P. 2015. *Design-Expert®*. Minneapolis, Minnesota: Stat-Ease, Inc.
- Wilczewska, A. Z., Niemirowicz, K., Markiewicz, K. H. & Car, H. 2012. Nanoparticles as drug delivery systems. *Pharmacological Reports*, 64, 1020-1037.
- Yan, M., Zhang, Y., Xu, K., Fu, T., Qin, H. & Zheng, X. 2011. An in vitro study of vascular endothelial toxicity of CdTe quantum dots. *Toxicology*, 282, 94-103.
- Yang, S.Y., Zheng, Y., Chen, J.Y., Zhang, Q.Y., Zhao, D., Han, D.E. & Chen, X.J. 2013. Comprehensive study of cationic liposomes composed of DC-Chol and cholesterol with different mole ratios for gene transfection. *Colloids and Surfaces B: Biointerfaces*, 101, 6-13.
- Zhang, X., Yang, S., Zhang, H., Yang, Y., Sun, S., Chang, J., Tao, X., Yang, T., Liu, C. and Yang, Y. 2015. Endoplasmic reticulum stress mediates the arsenic trioxide-induced apoptosis in human hepatocellular carcinoma cells. *The International Journal of Biochemistry & Cell Biology*, 68, pp.158-165.
- Zhang, X.Q., Intra, J. & Salem, A. K. 2007. Conjugation of polyamidoamine dendrimers on biodegradable microparticles for nonviral gene delivery. *Bioconjugate Chemistry*, 18, 2068-2076.
- Zhang, X., Qi, J., Lu, Y., He, W., Li, X. & Wu, W. 2014. Biotinylated liposomes as potential carriers for the oral delivery of insulin. *Nanomedicine: Nanotechnology, Biology and Medicine*, 10, 167-176.